The Effects of Fructose Feeding on the Quantal Catecholamine Release from Adrenal Chromaffin Cells

by

Weixiao Zhao

A thesis submitted in partial fulfillment of the requirements for the degree of

Master of Science

Department of Pharmacology
University of Alberta

Abstract:

Adrenal chromaffin cells release catecholamines in response to stress, via the exocytosis of large-dense core granules (LDCGs). Excessive stress responses, however, are harmful and can lead to the development of hypertension. The fructose-fed rats, an animal model with the symptom of hypertension, exhibit an elevated plasma catecholamine level. The object of my study was to test the hypothesis that fructose feeding may enhance the efficiency of quantal release of catecholamines from individual chromaffin cells. Carbon fiber amperometry was employed to detect quantal catecholamine release from chromaffin cells. When cells were stimulated by carbachol, a non-selective cholinergic agonist that robustly activates both muscarinic and nicotinic receptors, fructose feeding increased the amount of catecholamine released per cell as well as per individual events of exocytosis (i.e. the quantal size, Q). When cells were stimulated by dimethylphenylpiperazinium (DMPP), a selective nicotinic receptors agonist, fructose feeding caused an increase in cellular secretion which was associated with an increase in the number of events of exocytosis per cell and a smaller increase in Q. In contrast, both the carbachol and DMPP-evoked Ca^{2+} signals were reduced by fructose feeding. The following scenario may account for the above findings: fructose feeding recruited a population of granules with intermediate Q, resulting in an increase in the number of granules that underwent exocytosis when stimulated with nicotinic agonist. The co-activation of muscarinic and nicotinic receptors promoted some form of granule-granule fusion, resulting in the exocytosis of large Q granules which have more rapid release kinetics. My overall results suggest that fructose feeding enhances the secretion of catecholamine from rat chromaffin cells upon cholinergic stimulation. The augmentation of adrenal catecholamine release can contribute to the development of hypertension induced by high fructose consumption.

Table of Contents: **Page(s)**

List of tables: **Page(s)**

Chapter 3:

Appendix:

List of figures: **Page(s)**

Chapter 1:

Chapter 2:

Chapter 3:

Abbreviations List:

ACh	Acetylcholine
AChR	Acetylcholine receptor
BSA	Bovine serum albumin
CNS	Central nervous system
DMEM	Dulbecco's modified Eagle's medium
DMPP	Dimethylphenylpiperazinium
DMSO	Dimethyl sulfoxide
Epac	Exchange protein directly activated by cAMP
ER	Endoplasmic reticulum
Fura-2 AM	Fura-2-acetoxymethyl ester
GPCR	G-protein coupled receptor
HPLC	High pressure liquid chromatography
IP_3	Inositol 1,4,5-trisphosphate
IP_3R	IP_3 receptor
ITS	Insulin-transferrin-selenium
LDCG	Large dense core granule
mAChR	Muscarinic acetylcholine receptor
MEM	Minimal essential media
nAChR	Nicotinic acetylcholine receptor
PKC	Protein kinase C
PSF	Pre-spike foot

Q	Quantal size
ROS	Reactive oxygen species
SNAP-25	Synaptosomal-associated protein 25
SNARE	Soluble N-ethylmaleimide-sensitive factor attachment protein receptor
VGCC	Voltage-gated Ca^{2+} channel

Chapter 1 Introduction

1.1 *The Stress Response and Stimulus-Secretion Coupling in Adrenal Chromaffin Cells*

Chromaffin cells of the adrenal medulla play a crucial role in the "fight-or-flight" stress response by secreting catecholamines into the bloodstream (Kvetnansky et al., 2009). The catecholamines (mainly adrenaline and noradrenaline) in the circulation increase the heart rate, vascular tone, blood flow to the skeletal muscles and elevate the plasma glucose levels. These effects help to prepare the body to fight, or flight from, the stressor. Although the stress responses in short term are crucial for survival, excessive or chronic stress responses lead to elevations in plasma levels of catecholamine and are detrimental to health (Currie, 2010). For instance, increased catecholamine levels are implicated in the development of hypertension (Takiyyuddin et al., 1993) and contribute to the morbidity and mortality of chronic heart failure (Floras, 2003). *In situ*, chromaffin cells are innervated by splanchnic nerve terminals that release acetylcholine (ACh). Activation of the nicotinic acetylcholine receptors (nAChRs) and/or the muscarinic acetylcholine receptors (mAChRs) on the chromaffin cells lead to an increase of intracellular Ca^{2+} concentration ($[Ca^{2+}]_i$) which in turn triggers the catecholamine-containing large dense core granules (LDCG) to undergo exocytosis (Wu et al., 2010;Fenwick et al., 1982;Forsberg et al., 1986;Kao and Schneider, 1985;Kilpatrick et al., 1982). Specifically, the activation of nAChRs induces the influx of extracellular Na^+ and Ca^{2+} through the nAChR channels. The influx of cations causes membrane depolarization, which opens voltage-gated Ca^{2+} channels (VGCCs) and allows the entry of more extracellular Ca^{2+}. On the other hand, the activation of mAChRs triggers Ca^{2+} release from intracellular Ca^{2+} stores; the stimulation of G_q coupled mAChRs activates phospholipase C and results in the generation of diacylglycerol and inositol 1,4,5-trisphosphate (IP_3). IP_3 binds to IP_3 receptors (IP_3Rs) in the endoplasmic reticulum (ER) and triggers intracellular Ca^{2+} release. As a Ca^{2+} source, the ER's contribution to $[Ca^{2+}]_i$ rise is small, thus the

catecholamine secretion induced by mAChRs activation is less in comparison to that of nAChRs. However, it has been suggested that mAChRs activation may contribute to the prolonged and sustained phase of secretion (Wu et al., 2010).

1.2 *Modulations of regulated exocytosis in chromaffin cells*

In chromaffin cells, the majority of secretory granules are restricted from the plasma membrane by a dense cytoskeletal network composed predominantly of actin (Burgoyne and Morgan, 1993;Trifaro and Vitale, 1993), such granules are considered to be the reserve pool. There is a small population of granules that are in close proximity to the plasma membrane. These granules are docked and primed, can undergo Ca^{2+}-triggered exocytosis rapidly, and thus are considered to be the readily-releasable pool (Morgan and Burgoyne, 1997). When chromaffin cells are stimulated, the resultant increase in $[Ca^{2+}]_i$ triggers the granules in the readily-releasable pool to fuse rapidly with the plasma membrane. Meanwhile, the $[Ca^{2+}]_i$ rise also aids in the mobilization of granules from the reserve pool to replenish the readily-releasable pool by causing disassembly of the cortical actin barrier (Morgan and Burgoyne, 1997) as well as the downstream steps of priming (Klenchin and Martin, 2000).

Exocytosis can be modulated in different steps of the stimulus-secretion coupling such as the modulation of Ca^{2+} signal, and/or the modulation of exocytotic machinery which include the changes in protein-protein interactions and the properties of the fusion pore. For example, the VGCCs in chromaffin cells can be reduced by the activation of G-protein coupled receptors (GPCRs) whose $G_{\beta\gamma}$ subunits bind directly to the α_1 subunit of the channel (Currie, 2010). This mechanism underlies the reduction of total Ca^{2+} current in chromaffin cells when the opioid or P_{2Y} purinergic receptors were activated (Chen et al., 2005;Currie, 2010). Since the LDCG of chromaffin cells also store and secrete opioids and ATP along with catecholamines, the inhibition of Ca^{2+} channels through the activation of opioid and P_{2Y} purinergic

receptors may underlie a potent feedback inhibition on catecholamine secretion (Currie, 2010). Different types of Ca^{2+} channels in chromaffin cells are recruited by various physiological or pathophysiological stressors, and some studies have shown that the activation of different types of Ca^{2+} channels can preferentially trigger certain pools of granules (Artalejo et al., 1994;Engisch and Nowycky, 1996;Lukyanetz and Neher, 1999;Alvarez et al., 2008). Via this mechanism, a large repertoire of patterns of secretion can be initiated in response to a wide range of stressors.

For a mature LDCG in the readily-releasable pool to fuse with the plasma membrane and release catecholamine, it has to be first docked to the membrane by forming a SNARE (soluble N-ethylmaleimide-sensitive factor attachment protein receptor) complex between the vesicular and plasma membrane (Becherer et al., 2012). The core of the SNARE complex is composed of three proteins: syntaxin and SNAP-25 (Synaptosomal-associated protein 25) on the plasma membrane along with synaptobrevin on the vesicular membrane. Conformational changes in the SNARE complex are proposed to provide the energy which drives the two membranes to merge; thus the SNARE complex is considered to be the core fusion machinery (Becherer et al., 2012). Other proteins are associated with, and regulate the conformation of, the SNARE complex. For example, a key Ca^{2+} sensor of the SNARE complex is synaptotagmin 1 on the vesicle membrane which binds Ca^{2+} to triggers exocytosis (Becherer et al., 2012). Besides the SNARE complex and proteins associated with it, numerous other proteins are reported to modulate various steps in the process of exocytosis. For example, studies have suggested that Ca^{2+}-dependent protein kinase C (PKC) activation may facilitate catecholamine secretion in chromaffin cells (Smith, 1999). PKC activation can also increase secretion via increasing the size of the readily-releasable pool and facilitating the recruitment of granules (Nagy et al., 2002;Gillis et al., 1996).

The final steps of exocytosis start with the formation of a fusion pore where the

lumen of the granule forms a transient connection with the extracellular environment. There is strong evidence to support the idea that the fusion pore is formed when a conformational change in a ring of SNARE complexes bend and fuse the lipids in the vesicular and plasma membranes (Burgoyne and Morgan, 2003;Rettig and Neher, 2002). In many secretory cell types, the opened fusion pore typically undergoes rapid dilation (within a few milliseconds) to allow significant release and subsequent depletion of vesicular content but other modes of exocytosis have also been identified (see Section 1.3). Fluctuation of the initial fusion pore can affect both the release property of granules and the amount of catecholamine released per fusion event. For example, changes in membrane lipid composition such as cholesterol perturbation can alter fusion pore kinetics by affecting its stability and the exocytotic process (Zhang et al., 2009;Wang et al., 2010).

1.3 *Exocytotic events detection by amperometry*

Amperometry is widely used to study the process of exocytosis for its excellent temporal resolution and its ability for the quantification of neurotransmitter release (Mosharov and Sulzer, 2005). For detection of quantal release of catecholamine transmitter or hormone, carbon fiber amperometry has been frequently employed. In this method, a carbon fiber electrode is voltage clamped at a positive potential (+700 mV) and is positioned against the surface of a secretory cell. The fusion of individual secretory granules is detected as spike-like amperometric signals (Fig. 1.1) that are generated from the oxidation of the monoamine molecules released from the granules. The analysis of these spikes (e.g. the kinetic parameters) can provide important information on the molecular steps involved in exocytosis (Mosharov and Sulzer, 2005).

The secretory granules in chromaffin cells can fuse with the plasma membrane via two alternative modes: full fusion and “kiss-and-run”. Full fusion occurs when the initial opening of the fusion pore is followed by an abrupt dilation that leads to the

complete merger between granule and plasma membrane and the release of the majority of catecholamine packaged within the granule (Fig. 1.2a). The majority of full fusion spikes are preceded by a pre-spike "foot" signal (PSF), revealing the leakage of catecholamine from the fusion pore before the onset of its rapid dilation (Zhou et al., 1996;Chow et al., 1992) (Fig. 1.2b). Alternatively, an extreme form of the kiss-and-run mode is detected as a stand-alone foot signal (Fig. 1.2c) which reflects a transient fusion pore that flickers (for up to tens of milliseconds) after opening and then closes without undergoing full expansion. Such stand-alone foot signals may also cause partial release of vesicular catecholamine because of the limited size and open time of the fusion pore (Zhou et al., 1996;Toledo G. et al., 1993;Elhamdani et al., 2001).

Because every molecule of the released catecholamine will be oxidized at the tip of the carbon fiber into 2 electrons (Gong et al., 2003), the time integral of the current of each individual amperometric spike can be used to estimate the amount of catecholamine released per granule (Q, or the quantal size) (Gong et al., 2003). As summarized in Fig. 1.3, other details of quantal release of catecholamine can be documented from the kinetic parameters of individual amperometric signals. These parameters include the spike amplitude (which reflects the maximum rate of catecholamine release from the dilated fusion pore), the spike rise time (which is the duration between 50 to 90% of the spike rising phase and reflects how quickly catecholamine is released after the onset of fusion pore dilation), the half width (the duration at 50% of the peak), spike amplitude and the decay time constant (τ) of the spike (which is fitted from the exponential decay phase). The last three parameters (spike rise time, half width and decay τ) reflect how quickly catecholamine is released and depleted after the fusion pore has started to dilate rapidly (Fig. 1.3). For the prespike foot (PSF) signals, foot amplitude reflects the size of the fusion pore. The foot duration is the time while the fusion pore's at its semi-stable state before its rapid dilation and reflects the stability of the fusion pore.

1.4 *A diet-induced model of hypertension: the fructose-fed rat*

Metabolic syndrome is a complex metabolic disorder that is characterized by hyperglycemia, hyperinsulinemia, dyslipidemia, central obesity and hypertension (Tran et al., 2009;Wajchenberg et al., 1994). Patients with metabolic syndrome are predisposed to the development of cardiovascular disorders and type 2 diabetes (Hanson et al., 2002;Lorenzo et al., 2003). As a diet-induced model of metabolic syndrome, the fructose-fed rat acquires systolic hypertension along with other features of the metabolic syndrome including high plasma levels of insulin, triglyceride and insulin resistance (Hwang et al., 1987;Panchal and Brown, 2011;Tran et al., 2009). Since high fructose feeding for 4-8 weeks does not result in weight gain (Tran et al., 2009), the fructose-fed rat is extensively employed to study the development of hypertension independent of obesity and genetic factors.

The amount of fructose and the duration of the fructose-enriched diet required to induce hypertension in rat have been studied extensively. In one study, male Sprague-Dawley rats were fed on a 66% fructose-enriched diet for 12 weeks, their systolic blood pressure started to increase after 2 weeks of feeding and peaked at the 8^{th} week. The elevation in systolic blood pressure persisted between the 8^{th} and the 12^{th} week of fructose feeding. There was no excess weight gain with fructose feeding over the 8 week period. However, from the 10^{th} week, the fructose-fed rats started to show an increase in weight (Chen et al., 2009). In the 6-week fructose feeding protocol used by laboratories of Professors Alexander Clanachan and Michael Zaugg (Department of Pharmacology) (Lou et al., 2015;Warren et al., 2014), male Sprague-Dawley rats received a standard rodent diet with 10% fructose in the drinking water, equivalent to a diet in which fructose comprise ~50% of the calories (Warren et al., 2014). After 6 weeks of fructose feeding, these rats consistently exhibited hyperglycemia, hyperinsulinemia, hypertriglyceridemia, insulin resistance and arterial hypertension (Warren et al., 2014;Lou et al., 2015). Specifically, at the

end of 6th week, the fructose-fed rats exhibited an increase of ~ 30 mm Hg in both systolic and diastolic blood pressures (Warren et al., 2014).

1.5 *The possible mechanisms of fructose-induced hypertension*

The literature suggests that the development of hypertension in fructose-fed rats may be mediated by a change in the activity of the sympathetic nervous system (Verma et al., 1999;Tran et al., 2009). In fructose-fed rats, adrenal medullectomy followed by weekly injections of 6-hydroxy dopamine (an isomer of noradrenaline which selectively abates the adrenergic sympathetic neuron signaling), prevented the development of both hyperinsulinemia and hypertension, indicating that the presence of a functional sympathetic nervous system is required for the development of fructose feeding induced hyperinsulinemia and hypertension (Verma et al., 1999). Interestingly, the addition of clonidine (an α_2 agonist that selectively suppresses the vasomotor centre in the CNS (central nervous system) which in turn inhibits the activity of, and the peripheral release of catecholamine from the sympathetic nervous system) to the drinking water reversed the fructose-induced hypertension in rats, without affecting hyperinsulinemia and hypertriglyceridemia (Hwang et al., 1987). A more recent study by Hsien and Huang (2001) examined the role of the peripheral sympathetic nervous system in the fructose-induced hypertensive rats. When neonatal rats were injected with guanethidine (a false transmitter that replaces noradrenaline in the vesicles of post-ganglionic adrenergic neurons), the fructose-induced elevations in blood pressure and plasma triglyceride levels (Hsieh and Huang, 2001) were attenuated, but not prevented. This study suggests that the peripheral sympathetic nervous system is involved in the development of hypertriglyceridemia and hypertension induced by fructose feeding.

Fructose feeding also increased the urinary excretion of adrenaline and noradrenaline in rats (Kamide et al., 2002). Since the source of adrenaline in the circulation arises primarily from the adrenal medulla, the elevation in urinary

excretion of adrenaline in the fructose-fed rats suggests that fructose feeding may increase the secretion of catecholamines from adrenal medulla. One possible mechanism that can contribute to the increase of secretion is an increase in catecholamine synthesis and storage in the adrenal medulla. However, using high pressure liquid chromatography (HPLC) and electrochemical detection of bioamines, a former master's student from our laboratory (Michael Simpson) has found that the total cellular content of catecholamine and the ratio of adrenaline to noradrenaline were unchanged in the adrenal medulla of fructose-fed rats. Nevertheless, in a study with a genetic hypertensive rat model, the spontaneous hypertensive rats, the quantal size of granules and the overall secretion of catecholamines from adrenal chromaffin cells were increased (Miranda-Ferreira et al., 2008). Specifically, in response to ACh or high K^+ stimulation, more granules in chromaffin cells from the spontaneous hypertensive rats underwent exocytosis and these granules had a bigger quantal size and faster release kinetics.

1.6 *Objective and hypothesis*

The observations in the spontaneous hypertensive rats raised the possibility that fructose feeding may augment catecholamine secretion from chromaffin cells independent of any increase in sympathetic tone. Therefore, in my thesis research, my objective was to determine whether chromaffin cells isolated from fructose-fed rats secreted more catecholamines in comparison to controls when they were activated by the same strength of pharmacological stimulation. I shall test the hypothesis that fructose feeding enhances the efficiency of quantal release of catecholamines from individual chromaffin cells.

Figures:

Figure 1.1:

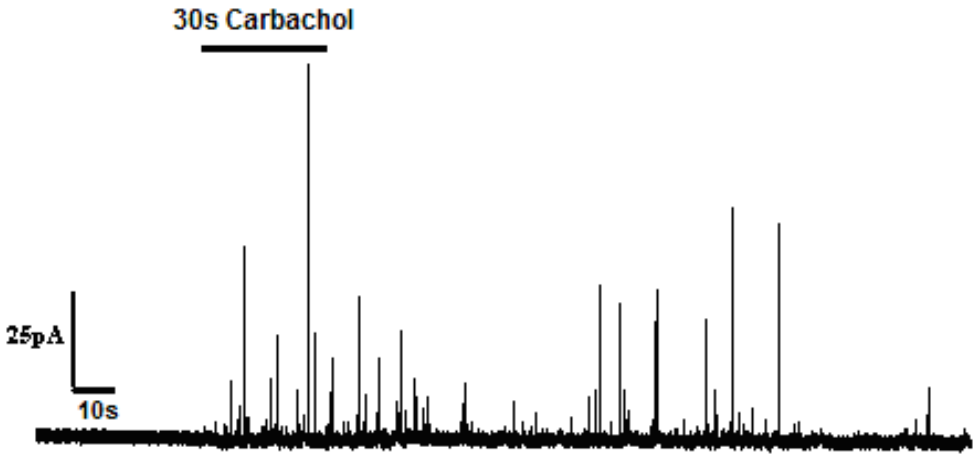

An example of a 3 min 40 s recording of a control chromaffin cell stimulated with carbachol (1 mM) for 30 s. Bursts of spike-like amperometric signals were evoked following carbachol stimulation.

Figure 1.2:

a Footless spike

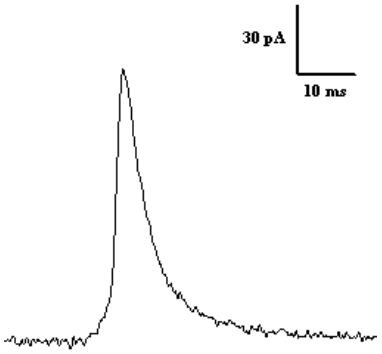

b Spike with a foot

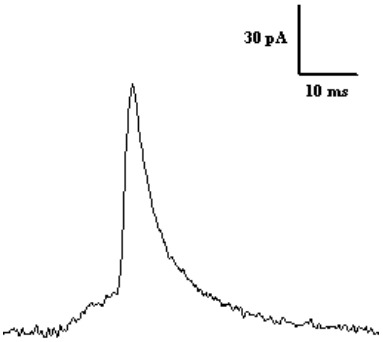

c "Stand-alone foot" signal

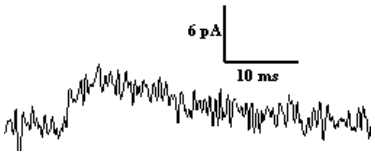

Examples of amperometric signals recorded from chromaffin cells. Full fusion of granules can be detected as either (a) a footless spike-like signal, or (b) a main spike with a pre-spike foot signal (PSF); (c) The "stand-alone foot" signal reflects catecholamine release from a granule through a semi-stable fusion pore, which flickers and may close before any significant dilation. This mode of release is also termed "kiss-and-run".

Figure 1.3:

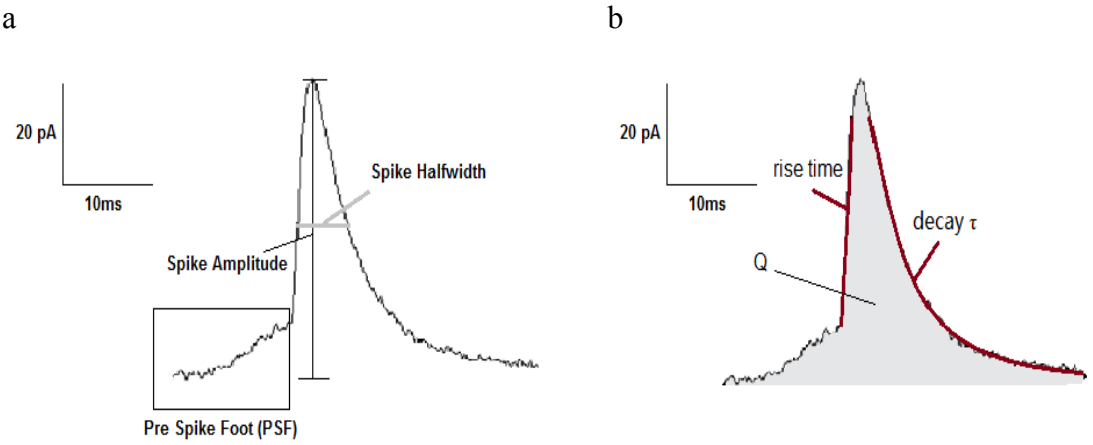

The kinetic parameters of individual amperometric signals. (a) The spike amplitude reflects the maximum rate of catecholamine release from the dilated fusion pore.
The spike halfwidth, is evaluated at 50% of the spike amplitude. (b) The amount of catecholamine released during an exocytotic event, Q, is estimated from the spike area. The rise time, is calculated as the time duration between 50% to 90% of the rising phase. The decay phase is fitted by an exponential with the time constant τ.

Chapter 2 Materials and Methods:

2.1 *Chemicals*

Carbachol, muscarine, dimethylphenylpiperazinium (DMPP), bovine serum albumin (BSA) and all the enzymes for cell dissociation (collagenase type I, hyaluronidase type I-S, deoxyribonuclease type I, and trypsin type I) were purchased from Sigma-Aldrich Ltd. (Oakville, ON, Canada). Dulbecco's modified Eagle's medium (DMEM), minimal essential media (MEM), insulin-transferrin-selenium (ITS), penicillin, streptomycin were obtained from Gibco (Grand Island, NY, USA). D-fructose was purchased from Alfa Aesar (Ward Hill, MA, USA). Fura-2-acetoxymethyl ester (Fura-2 AM) was from Invitrogen (Eugene, OR, USA).

2.2 *Animals and diets*

Male Sprague-Dawley rats at the age of 5 weeks were obtained from the Bioscience Animal facility at the University of Alberta. All rats were housed under a 12-h light/dark cycle at room temperature for 1 week before divided into two groups: control and fructose-fed. Using the fructose feeding protocol adapted from the one used by the laboratories of Professors Alexander Clanachan and Michael Zaugg (Department of Pharmacology) (Lou et al., 2015;Warren et al., 2014), the control group received a standard rodent diet and regular drinking water while the fructose-fed group received a fructose-enriched diet (standard rodent diet and 10% fructose added to the drinking water) for 6 weeks. This fructose-enriched diet was equivalent to a diet where ~50% of the calories are derived from fructose (Warren et al., 2014). According to the measurements carried out in the laboratories of Drs. Clanachan and Zaugg, after 6 weeks of fructose feeding, rats consistently exhibited hyperglycemia, hyperinsulinemia, hypertriglyceridemia, insulin resistance, arterial hypertension, and abdominal obesity. Specifically, the fructose-fed rats exhibited an

increase of ~ 30 mmHg in both systolic and diastolic blood pressures at the end of the 6th week (Warren et al., 2014). In my experiments, all experimental animals were used within 5 days after the 6^{th} week of fructose feeding and the fructose-fed rats were compared with their age matched controls.

2.3 *Preparation of chromaffin cell cultures*

Primary cultures of dissociated chromaffin cells were prepared from rat adrenal glands as described previously (Xu and Tse, 1999;Tang et al., 2005). Briefly, male Sprague-Dawley rats (~12 weeks old) were euthanized by intraperitoneal injection of euthanyl in accordance with the standards of the Canadian Council on Animal Care. The adrenal glands were removed and kept in cold sterilized HEPES buffer solution (NaCl: 137 mM, KCl: 5 mM, $Na_2HPO_4 \cdot 7H_2O$: 0.7 mM, glucose: 10 mM, Hepes: 25 mM, penicillin G: 50 U/ml and streptomycin: 50 μg/ml). The adrenal medullas were dissected out, with surrounding tissues trimmed off and washed three times with HEPES buffer. The adrenal medullas were then incubated in a collagenase solution containing collagenase type I (3.0 mg/ml), hyaluronidase type I-S (2.4 mg/ml), and deoxyribonuclease type I (0.2 mg/ml) for 25-30 minutes at 37°C. The solution was gently shaken every 5 min to make sure that the tissue pieces were not clumped together. The tissue suspension was centrifuged at 2800 rpm for 4 min and the supernatant was removed. The tissue pellet was then washed with HEPES buffer and triturated with a Pasteur pipette with a fire polished tip for 20-30 times. After another round of 20-30 times trituration with a finer polished Pasteur pipette, the tissue was further digested by incubating with a trypsin solution (trypsin type I 1 mg/ml) at 37°C for 5 min. Dulbecco's modified Eagle's medium supplemented with 0.5% of bovine serum albumin (DMEM-BSA) solution was then added to the tissue solution. After centrifugation and the removal of the supernatant, the tissue pellet was washed with DMEM-BSA two times. Following centrifugation, the cell pellet was resuspended in DMEM-BSA. A droplet of 10 μl of the cell suspension was plated onto each glass cover slip placed in 35 mm diameter plastic Petri dishes. The Petri dishes were then

kept at 37°C in a water-saturated incubator with a 5% CO_2 - 95% air atmosphere for 45 min to 1 h to allow the cells to settle down. Each dish was then flooded with 2 ml of MEM supplemented with 1% (v/v) insulin-transferrin-selenium, 50 U/ml penicillin G and 50 μg/ml streptomycin (MEM-ITS). Cells were kept in the incubator for 1.5 - 4 hours before experiment.

2.4 *Amperometry and signal analysis*

Amperometry with carbon fiber electrodes was performed on single chromaffin cells to detect catecholamine quantal release as described previously (Xu and Tse, 1999;Tang et al., 2005). Carbon fiber electrodes were made according to procedures modified from Zhou and Misler et al (Zhou and Misler, 1995;Zhou et al., 1996). A single carbon fiber with a diameter of 7 μm was carefully threaded into an Eppendorf micro-pipette tip (volume of <10 μl). The fiber-loaded pipette was then placed on a homemade micropipette puller. The pipette was positioned such that its narrow tip was near a heating element. Once the heating element was heated up, the narrow tip of pipette started to melt. The plastic became transparent and a bead-like shape was formed. At this point, tension was applied to gently stretch the plastic, leaving the exposed carbon fiber insulated with a thin layer of plastic. The carbon fiber exposed in the center region was transected with a scalpel blade. This resulted in a carbon fiber electrode with an un-insulated carbon fiber tip. A certain length of fiber was left extending into the pipette such that there was sufficient conductive contact to be attached to the head stage of an amplifier via a 4 M NaCl filling solution (Zhou and Misler, 1995;Zhou et al., 1996).

The experimental configuration was set up as described previously (Xu and Tse, 1999;Tang et al., 2005) (Fig. 2.1). All experiments were conducted at room temperature. Individual cover slip with cells was mounted onto the recording chamber (ALA Scientific Instruments, Farmingdale NY) in which the coverslip forms the bottom of the chamber. The chamber was perfused with Normal Ringer's solution that contained the following (in mM): 150 NaCl, 2.5 KCl, 2 $CaCl_2$, 1 $MgCl_2$, 8 glucose, 10

Hepes (adjusted to pH 7.4 with NaOH) via a local perfusion pipette positioned near the cell of interest. The carbon fiber electrode was voltage clamped to +700 mV via a VA10 amplifier (NPI Electronics; Tamm, Germany) and was positioned to gently touch the cell surface. The cells were stimulated to release catecholamines via switching the local application of Normal Ringer's solution to one containing an acetylcholine agonist (carbachol: 1 mM or 0.1 mM; DMPP: 0.1mM; or muscarine: 0.1mM) dissolved in Normal Ringer's solution. For all experiments, data was collected for 3 min 40 s where the first 40 s was a baseline recording followed by a 30 s application of agonist, and then 2 min 30 s of wash with Normal Ringer's solution (Fig. 2.1). Each catecholamine molecule released during exocytosis was oxidized by the highly positively charged carbon fiber electrode. The 2 electrons generated from the oxidation of the catecholamine were detected as a current by the amplifier. The unfiltered output of the amplifier was then low passed at 1 kHz by an 8-pole Bessel filter (Frequency Device) and digitized at 10 kHz with a Digidata 1332A running on the pClamp software (Molecular Devices). A typical amperometric signal was depicted in Fig. 2.1, identifying the fusion event of an individual dense core granule.

Amperometric signals were first detected by screening all signals whose amplitude was >3×rms noise of the baseline. Then the non-overlapping signals were selected by visual inspection before analyzed with the Mini Analysis Program version 6.03 (Synaptosoft Inc., Decatar, Geogia, USA). The analysis was restricted to individual amperometric signals using the same criteria described in our previous studies (Xu and Tse, 1999;Tang et al., 2005): (1) the 50%-90% rise time must be < 5 ms; (2) the decay time constant (τ) must be <40 ms; (3) the interval between the peaks of two adjacent events must be > 3 times the decay time constant of the first event; (4) the area must be > 10 fC; and (5) the half width must be greater than 1 ms (Xu and Tse, 1999;Tang et al., 2005). Origin 7.5 (OriginLab Corporation, Northampton, Massachusetts, USA) was used for further data processing. For every cell, the mean values of the kinetic parameters of all amperometric events were obtained. Then a mean of cellular mean was calculated among all the cells in each experimental

condition. The two populations Student's *t* test was used when comparing between the mean of cellular mean values of cells between two groups of cells in different experimental conditions. Values of $p < 0.5$ were considered statistically significant and marked with asterisks in the figures and tables. When comparing the cumulative $Q^{1/3}$ distribution between different experimental conditions, the Kolmogorov-Smirnov (K-S) test included in the Mini Analysis Program was used to determine the statistical significance of difference. When comparing the kinetic parameters at matched narrow ranges of $Q^{1/3}$ between cells in different experimental conditions, the two populations Student's *t* test was used. Values shown in the text, figures and tables are mean ± standard errors (SE).

2.5 *Calcium Imaging*

Free cytosolic Ca^{2+} concentration ($[Ca^{2+}]_i$) was measured using the fluorescent Ca^{2+} indicator, fura-2-acetoxymethyl ester (fura-2 AM). Individual glass coverslip plated with chromaffin cells was mounted into a recording chamber. Then 0.5 ml of Normal Ringer's solution supplemented with 0.5 ml of 5 μM fura-2AM (dissolved in dimethyl sulfoxide (DMSO) was added to the cells, and incubated at 37°C in the dark for 15 min. Fura-2 is a ratiometric dye which has an emission peak at 510 nm and changes its excitation peak from 340 nm to 380 nm in response to Ca^{2+} binding. Therefore, the concentration of Ca^{2+} can be quantified by comparing the 340 nm/380 nm fluorescence ratio.

After incubation with fura-2AM, the cells were perfused with Normal Ringer's solution at room temperature. $[Ca^{2+}]_i$ was monitored with digital imaging using a Tillvision imaging system equipped with Polychrome II high speed monochromator (Applied Scientific Instrument, Eugene, OR, USA). Fura-2 was excited sequentially by 340 and 380 nm light delivered from a xenon lamp via a 40x, 1.3 NA UV fluor oil immersion objective objective (Olympus). Fluorescent images were collected via a

cooled CCD camera every 5 s. In all Ca^{2+} imaging experiments, cells were perfused with the Normal Ringer's solution during the first 40 s, followed by a 30 s application of an cholinergic agonist dissolved in Normal Ringer's solution and then a 2 min 30 s of wash with Normal Ringer's solution. The ratio of the fluorescence, 340 nm/380 nm from individual cell was analyzed with the aid of Tillvision Software 3.02 (Applied Scientific Instrument) on an IBM-compatible computer.

Figures:

Figure 2.1:

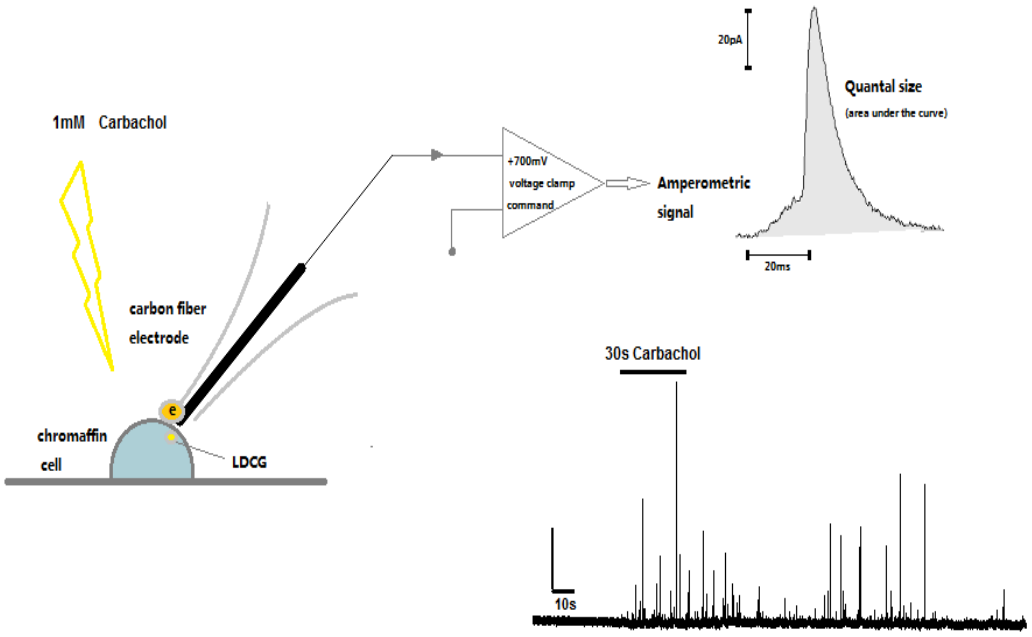

The experimental configuration of carbon fiber amperometry. The carbon fiber electrode (voltage clamped at +700 mV) was positioned to gently touch the cell surface. A baseline recording of 40 seconds was made when the cell was perfused with Normal Ringer's solution. The cell was then stimulated by a 30 seconds of cholinergic agonist, e.g. carbachol, to release catecholamine. Another 2 min 30 s of recording was made during the wash off with Normal Ringer's solution. The exocytosis of individual granules was detected as spike-like currents. The integral of each amperometric signal which is the area under the spike, represents the amount of catecholamine released from the fusion of that granule.

Chapter 3 Results:

3.1 *Fructose feeding augmented the total amount of catecholamine secretion from individual cells via an increase in the quantal size of granules when stimulated by 1 mM carbachol*

In situ, chromaffin cells in the adrenal medulla are innervated by cholinergic nerve terminals of the splanchnic nerve. Acetylcholine (ACh) released by the splanchnic nerve terminals activates the acetylcholine receptors (AChRs) on the chromaffin cell membrane. The activation of these receptors then elevates $[Ca^{2+}]_i$ which triggers the catecholamine-containing large dense-core granules to undergo exocytosis. To mimic the effects of cholinergic stimulation, I first employed the non-selective cholinergic agonist, carbachol which is resistant to cholinesterase. When compared to ACh, carbachol is an agonist with lower potency and efficacy (Schneider et al., 1977). Moreover, ACh was detected at a concentration as high as 1 to 10 mM near its release site (Smart and McCammon, 1998;Matthews-Bellinger and Salpeter, 1978;Kleinle et al., 1996). When I stimulated chromaffin cells with 1 mM carbachol, typically ~70 amperometric events could be detected from a single cell. However, when the concentration of carbachol was reduced to 0.1 mM, only ~40 events were observed. In order to elicit a robust response in catecholamine release, I have employed 1 mM carbachol in my study. The saturating concentration of carbachol employed here also allows me to address specifically whether fructose feeding can further augment catecholamine secretion under maximum cholinergic stimulation.

Carbon fiber amperometry was applied to monitor the carbachol-induced catecholamine secretion. When cells were perfused with Normal Ringer's solution, as in the first 40 s of baseline recording (see Fig. 3.1a; same trace as shown in Fig. 2.1), they had no, or a very low rate of, spontaneous catecholamine quantal release; note that during this period in Fig. 3.1a, no amperometric spike was detected. Similar to

the example shown in Fig. 3.1a, bursts of amperometric spikes were recorded within seconds of the carbachol application for the majority of cells. When stimulated by 1 mM carbachol, >90% of chromaffin cells from both the control and the fructose-fed group were responsive. For the control and the fructose-fed groups, 94.44 ± 2.33% (65 out of 68 cells) and 93.42 ± 2.22% (78 out of 84 cells) (p = 0.76) responded respectively to carbachol stimulation. The percentage of response described above was defined as the percentage of cells with at least one spike in their recording traces among all the cells tested. When 10 spikes were used as the criterion, the percentage of responsive cells in the control and fructose-fed groups dropped to 69.7 ± 2.94% (48 out of 68 cells) and 75.66 ± 6.22% (62 out of 84 cells) (p = 0.46), respectively. For both criteria, there was no significant difference in the percentage of responsive cells between the fructose-fed rats and their age-matched controls. In all subsequent analyses, only cells with ≥ 10 spikes when stimulated with cholinergic agonists were included.

Since in amperometry, two electrons were generated by the oxidation of each molecule of catecholamines (Mosharov and Sulzer, 2005), the time integral of each amperometric signal represents the amount of catecholamine released from the fusion of an individual granule (i.e. the quantal size, Q; Fig. 3.1b). The total charge of the amperometric currents from one entire trace then correlates to the amount of catecholamine secretion from a chromaffin cell during the time of recording. In my study, for every chromaffin cell with at least 10 amperometric signals, the area under each individual signal (including the overlapping ones that were not included in further kinetics analysis) was summed up to calculate the total charge of all amperometric currents during recording. This was done instead of integrating the entire amperometric trace due to the reason that the integral can be biased by small drifts in the baseline. For instance, in a trace with many amperometric signals, a small fluctuation of the baseline can give rise to an integral that is a negative number. Conversely, the integral of a baseline segment without any amperometric spike can result in a number that outweighs the sum of the integral of many individual

amperometric spikes. As shown in Fig. 3.2a, the amount of secretion from individual chromaffin cells in response to a 30 s application of carbachol (1 mM) in the fructose-fed group was 65% larger than that of the control cells (16.88 ± 2.55 pC in control versus 27.87 ± 2.98 pC in fructose-fed; $p<0.05$).

The increased catecholamine secretion caused by fructose feeding could be due to more granules fusing with the plasma membrane and/or larger amount of catecholamine released from each granule. To assess these possibilities, I examined the number of amperometric spikes (which reflects the number of granules that underwent exocytosis), and the quantal size (Q, which reflects the amount of catecholamine released from the exocytosis of an individual granule). As shown in Fig. 3.2c, the average number of amperometric spikes from individual cells triggered by 1 mM carbachol was unchanged by fructose feeding (71.83 ± 7.4 amperometric spikes/cell in control versus 75.81 ± 6.80 amperometric spikes/cell in fructose-fed, $p = 0.69$). In contrast, fructose feeding increased the mean cellular quantal size by ~70% (0.19 ± 0.01 pC in controls versus 0.32 ± 0.02 pC in fructose-fed; $p<0.05$; Fig. 3.2b). Note that the fractional increase of quantal size is similar to the increase in total secretion from each cell. This result shows that the fructose-induced increase in total cellular secretion was mainly due to the increase in the quantal size, rather than a change in the number of secretory granule undergoing exocytosis (Fig. 3.3).

There are several potential mechanisms underlying the increase in the quantal size associated with fructose feeding. An example is the switch in different modes of exocytosis (Zhou et al., 1996;Elhamdani et al., 2001). The secretory granules in neuroendocrine cells can fuse with the plasma membrane via the two alternative modes: full fusion and "kiss-and-run" (see Chapter 1, Section 1.3). Since less catecholamine is released during the kiss-and-run mode when compared with full fusion, one possible scenario is that the proportion of chromaffin granules that undergo kiss-and-run was reduced by fructose feeding. However, in response to 1 mM carbachol, the kiss-and-run mode of fusion (reflected by the stand-alone foot signal;

e.g. Fig. 1.2c) occurred at a very low frequency (< 2%) in cells from both control and fructose-fed rats. Thus, the shift in this mode of exocytosis is unlikely to account for the fructose-induced increase in quantal size.

Another way to increase the quantal size is to increase the amount of catecholamine packaged into individual granules. The increased storage of catecholamine in granules may result from an increase in cellular catecholamine synthesis. However, previous experiments done by a former MSc student in our laboratory (Michael Simpson) using HPLC and electrochemistry to quantify the amount of catecholamine contained in rat chromaffin cells have shown that there was no significant difference in the average total amount of catecholamine (normalized to the amount of cellular proteins) between control and fructose-fed rats. Furthermore, the ratio of adrenaline to noradrenaline was also unchanged by fructose feeding.

The mean value of the quantal size shown in Fig. 3.2b was obtained by taking the average of the cellular mean quantal size for a population of cells. In fact, individual amperometric spikes recorded from the same cell had a relatively wide range of quantal sizes (Tang et al., 2005). In a previous study from our laboratory (Tang et al., 2005), we found that at least three populations of granules (defined according to their modal quantal size) could be exocytosed from rat chromaffin cells. Therefore, I plotted the $Q^{1/3}$ distribution curve of all the granules detected from the chromaffin cells in the control group when stimulated with 1 mM carbachol. As shown in Fig. 3.4, the data could be reasonably described by the summation of three Gaussian distributions. This agrees with the previous finding by Tang et al (2005) and suggests that there might be three populations of granules with its modal Q located at 0.38, 0.52 and 0.72 $pC^{1/3}$. For these three populations of granules, I refer them as small, intermediate and large Q granules.

To obtain additional insights into the changes in quantal size after fructose feeding, I analyzed the fractional distribution of the values of $Q^{1/3}$ collected from all

the amperometric signals recorded from the control and fructose-fed groups. The distribution of $Q^{1/3}$ instead of Q was examined because the distribution of Q is too right skewed for parametric statistical analyses. Previous studies have shown that the value of $Q^{1/3}$ is roughly proportional to the radius of the granules, as the value of Q is roughly proportional to the vesicular volume (Tang et al., 2005). As shown in Fig. 3.5a, fructose feeding caused a right shift in the $Q^{1/3}$ distribution. More specifically, the right shift of the $Q^{1/3}$ distribution reflected a bigger proportion of granules with an intermediate and large Q exocytosed after fructose feeding. Fig. 3.5b shows that the cumulative $Q^{1/3}$ distribution from the fructose-fed group is significantly different from the control group (K-S test, $p< 10^{-4}$). Fig. 3.5b also shows that the intermediate and large Q granules ($Q^{1/3} \geq 0.6$ $pC^{1/3}$) made up ~25% of the total granules in the control group and this percentage increased to ~40% in the fructose-fed group (Fig. 3.5b). In the control group, the large Q granules ($Q^{1/3} \geq 0.8$ $pC^{1/3}$) made up ~8% of total granules and this percentage increased to 20% (Fig. 3.5b), that is more than two-fold, after fructose feeding. This analysis suggested that the fructose-induced increase in cellular mean quantal size was due to an increase in the proportion of intermediate and large Q granules that underwent exocytosis.

I documented whether the increase in Q after fructose feeding was accompanied by changes in other kinetic parameters of the amperometric signal (see Table 3.1). When cellular mean values were compared, fructose feeding significantly changed some kinetic parameters of the spike and pre-spike foot (PSF) signals. Fructose feeding significantly increased the amplitude of the spike and PSF by the same extent (~ 160%; spike amplitude of 16.50 ± 2.08 pA in control versus 43.87 ± 4.17 pA in fructose-fed; PSF amplitude of 5.91 ± 0.53 pA in control versus 15.42 ± 1.20 pA in fructose-fed; Fig. 3.6). Interestingly, fructose feeding also accelerated the rise time, half-width and the decay τ of the spike, all by a similar extent (~14%; rise time of 1.83 ± 0.06 ms in controls versus 1.60 ± 0.04 ms in fructose-fed, half-width of 7.63 ± 0.25 ms in control versus 6.64 ± 0.19 ms in fructose-fed; and decay τ of 15.10 ± 0.59 ms in control versus 13.32 ± 0.40 ms in fructose-fed; Fig. 3.7). Fructose feeding did

not change the duration of the PSF signal, but increased its amplitude and charge (foot area) by ~ 160% and ~120 % respectively (5.91 ± 0.53 pA in control versus 15.42 ± 1.20 pA in fructose-fed for foot amplitude; Fig. 3.6b, 16.05 ± 1.39 fC in control versus 34.01 ± 2.40 fC in fructose-fed for foot area; Fig. 3.8). The above pattern of changes suggests that fructose feeding did not affect the persistence of the fusion pore before its rapid dilation but catecholamine was released from individual granules at a faster rate during both the PSF and spike signal.

To examine if the fructose-induced changes in the kinetic parameters of amperometric signal were associated with certain subpopulation(s) of granules, the kinetic parameters were compared at narrow ranges of matched $Q^{1/3}$ values. For such a comparison, the data sets from both the control and fructose-fed groups were first sorted in an ascending order of $Q^{1/3}$, and then grouped with a bin width of 0.1 $pC^{1/3}$. Fig. 3.9a shows the spike amplitude at increasing values of $Q^{1/3}$. For the control group, the spike amplitude increased with $Q^{1/3}$ values. In contrast, the patterns for spike halfwidth (Fig. 3.9b), rise time (Fig. 3.9c) and decay τ (Fig. 3.9d) were more complicated. For small Q granules ($Q^{1/3}$ ranges up to ~0.5 $pC^{1/3}$), the spike halfwidth, rise time and decay τ increased with $Q^{1/3}$. At larger $Q^{1/3}$ values, the value of the spike halfwidth reached a plateau, while the rise time and decay τ sagged with further increase in $Q^{1/3}$ (Fig. 3.9b-d). When compared with the data in the control group, fructose feeding increased the spike amplitude in a large range of Q (Fig. 3.9a). For the spike halfwidth (Fig. 3.9b), rise time (Fig. 3.9c) and decay τ (Fig. 3.9d), fructose feeding shortened the values of these three parameters particularly for the large Q granules ($Q^{1/3}$ from ~0.65 to 1.05 $pC^{1/3}$). The above finding raises the possibility that fructose feeding induced an acceleration of the spike kinetics in granules with larger values of Q. Fructose feeding also accelerated the foot kinetics. As shown in Fig. 3.10, there was an increase in foot amplitude and shortening in the foot duration for the large Q granules.

Multiple parameters of exocytosis were reported to be regulated by the

magnitude and pattern of the Ca^{2+} signal. The increase in $[Ca^{2+}]_i$ which triggers exocytosis is caused by the influx of extracellular Ca^{2+} through agonist- or voltage-gated channels, or the release of Ca^{2+} from intracellular stores. Although the relation between secretion and $[Ca^{2+}]_i$ is not linear (Augustine and Neher, 1992;Dodge, Jr. and Rahamimoff, 1967), it is a general observation that a larger $[Ca^{2+}]_i$ rise triggers more secretion. A larger rise in $[Ca^{2+}]_i$ was also reported to increase Q (Elhamdani et al., 2001). To examine whether the fructose-induced increase in Q and secretion were due to a larger carbachol-evoked Ca^{2+} signal, I stimulated the cells with 1mM carbachol for 30 s and measured the time integral of the Ca^{2+} signal with fura-2 digital imaging. As shown in Fig. 3.11, the mean time integral of the Ca^{2+} signal was decreased by 32% in the cells from fructose-fed rats. Therefore the elevations in Q and secretion after fructose feeding was not caused by a larger rise in $[Ca^{2+}]_i$.

3.2 *Fructose feeding augmented the total amount of catecholamine secretion from individual cells via increases in both the quantal size and the number of granules exocytosed when stimulated with 100 μM DMPP*

In the experiments described in section 3.1, chromaffin cells were stimulated with 1 mM carbachol, which was expected to robustly activate both nicotinic and muscarinic receptors. To examine whether the effects of fructose feeding can be observed when the nicotinic receptors are selectively activated, I employed a selective nicotinic agonist, DMPP.

In control cells stimulated by 100 μM DMPP (30 s), the average amount of catecholamine secretion per cell (13.53 ± 1.89 pC by DMPP versus 16.88 ± 2.55 pC by carbachol; $p = 0.29$), quantal size (0.18 ± 0.01 pC by DMPP versus 0.19 ± 0.01 pC by carbachol; $p = 0.82$) and the number of events (65.65 ± 7.41 amperometric spikes/cell by DMPP versus 71.83 ± 7.40 amperometric spikes/cell by carbachol; $p = 0.56$) were similar to those stimulated by 1 mM carbachol (Fig. 3.12). Therefore, I employed 100 μM DMPP in the following experiments. I first examined the

DMPP-evoked Ca^{2+} signals. Fructose feeding decreased the mean time integral of the DMPP-evoked Ca^{2+} signal feeding by ~34% (Fig. 3.13). Thus, fructose feeding reduced the time integral of the DMPP or carbachol-evoked Ca^{2+} signal to a similar extent.

When stimulated by 100 μM DMPP, more than 10 amperometric spikes could be detected in 84.24% of the cells (49 out of 58 cells) in the control group and 89.36% (43 out of 48 cells) in the fructose-fed group ($p = 0.66$). Thus, fructose feeding did not change the percentage of cells responsive to nicotinic stimulation. As shown in Fig. 3.14, fructose feeding increased the mean cellular secretion of chromaffin cells evoked by DMPP by ~92% (13.53 ± 1.89 pC in control versus 25.94 ± 3.77 pC in fructose-fed; $p < 10^{-2}$). In cells stimulated with DMPP, fructose feeding also increased the quantal size by ~35% (0.18 ± 0.01 pC in controls versus 0.25 ± 0.02 in fructose-fed, $p = 0.001$) and the number of events by ~47% (65.65 ± 7.41 amperometric spikes/cell in controls versus 96.72 ± 12.84 amperometric spikes/cell in fructose-fed, $p = 0.03$) (Fig. 3.14). These observations suggested that an increase in both Q and the number of granules exocytosed contributed to the increase in total secretion. The pattern of fructose-induced increase in secretion with DMPP was different to that with carbachol. As summarized in Fig. 3.15, the increase in carbachol-evoked secretion by fructose feeding was mainly due to the increase in quantal size. In contrast, the increase in DMPP-evoked secretion by fructose feeding was the product of the increase in quantal size and the number of granules exocytosed.

In the fractional $Q^{1/3}$ distribution from cells stimulated with DMPP (Fig. 3.16a), fructose feeding caused a smaller right shift in comparison to what was observed with carbachol stimulation (Fig. 3.5a). Nevertheless, the K-S test indicates that the cumulative $Q^{1/3}$ distribution of the fructose-fed group is significantly different from that of the control group ($p < 10^{-4}$; Fig. 3.16b). Fig. 3.16b also shows that granules with a $Q^{1/3} \geq 0.6$ $pC^{1/3}$ comprised ~20% of the total granules triggered in the control

group and this percentage increased to 30% in the fructose-fed group. For granules with a $Q^{1/3} \geq 0.8$ $pC^{1/3}$, there was little difference between the control and the fructose-fed group when stimulated by DMPP (Fig. 3.16b). This result is in contrast to the finding in cells stimulated with carbachol, where fructose feeding increased the proportion of large Q granules to more than 2 folds of the controls (Fig. 3.5b).

When the cellular mean values of kinetic parameters of the amperometric signals triggered by 100 μM DMPP were compared (Table 3.2), fructose feeding caused no change in the PSF, but significantly increased the spike amplitude (17.49 ± 1.84 pA in control versus 24.28 ± 2.17 pA in fructose-fed) and shortened the spike decay τ (15.2 ± 0.4 ms in control versus 12.6 ± 0.5 ms in fructose-fed). As summarized in Fig. 3.17, with DMPP stimulation, fructose feeding only increased the spike amplitude and accelerated the spike decay. When the kinetic parameters of the amperometric spikes triggered with DMPP stimulation were compared at narrow ranges of matched $Q^{1/3}$ (Fig. 3.18), fructose feeding caused only a small but significant increase in the spike amplitude at $Q^{1/3} < 0.6$, and selectively shortened the rise time, half width as well as decay τ of the spike for granules with $Q^{1/3}$ between 0.4 and 0.6 $pC^{1/3}$. As shown in Fig. 3.19, in cells with DMPP stimulation, neither the foot amplitude nor foot duration was altered by fructose feeding. This pattern contrasts the data set with 1 mM carbachol as the stimulus, in which fructose feeding robustly increased the amplitude and accelerated the kinetics of both the PSF and the spike over a wider range of $Q^{1/3}$, particularly at $Q^{1/3} > 0.6$ (Fig. 3.10).

Tables:

Table 3.1:

Comparisons of the amperometric experimental results between the control and fructose-fed rats when chromaffin cells were stimulated with 1 mM carbachol. The data in the control group was averaged from 48 cells obtained from 4 animals and the data in the fructose-fed group was averaged from 62 cells obtained from 5 animals.

	Control	Fructose-fed	*p* value
secretion per cell (pC)	16.88 ± 2.55	27.87 ± 2.98	* $p < 10^{-2}$
number of non-overlapping events	71.83 ± 7.4	75.81 ± 6.80	$p = 0.69$
Q (pC)	0.19 ± 0.01	0.32 ± 0.02	* $p < 10^{-5}$
$Q^{1/3}$ ($pC^{1/3}$)	0.52 ± 0.01	0.61 ± 0.01	* $p < 10^{-5}$
spike amplitude (pA)	16.50 ± 2.08	43.87 ± 4.17	* $p < 10^{-5}$
spike rise time (ms)	1.83 ± 0.06	1.60 ± 0.04	* $p < 10^{-3}$
spike halfwidth (ms)	7.63 ± 0.25	6.64 ± 0.19	* $p < 10^{-2}$
spike decay τ (ms)	15.10 ± 0.59	13.32 ± 0.40	* $p = 0.01$
PSF amplitude (pA)	5.91 ± 0.53	15.42 ± 1.20	* $p < 10^{-5}$
PSF duration (ms)	5.24 ± 0.29	5.45 ± 0.26	$p = 0.58$
PSF area (fC)	16.05 ± 1.39	34.01 ± 2.40	* $p < 10^{-5}$

Note: For all tables and figures, statistic significance (p<0.05) was denoted in asterisks (*). The values shown here, in the figures as well as in the text were mean ±SE.

Table 3.2:

Comparisons of the amperometric experimental results between the control and fructose-fed rats when chromaffin cells were stimulated with 100 μM DMPP. The data in the control group was averaged from 49 cells obtained from 3 animals and the data in the fructose-fed group was averaged from 43 cells obtained from 3 animals.

	Control	Fructose-fed	*p* value
secretion per cell (pC)	13.53 ± 1.89	25.94 ± 3.77	* $p < 10^{-2}$
number of non-overlapping events	65.65 ± 7.41	96.72 ± 12.84	* $p = 0.03$
Q (pC)	0.18 ± 0.01	0.25 ± 0.02	* $p < 10^{-2}$
$Q^{1/3}$ ($pC^{1/3}$)	0.50 ± 0.01	0.56 ± 0.01	* $p < 10^{-2}$
spike amplitude (pA)	17.49 ± 1.84	24.28 ± 2.17	* $p = 0.02$
spike rise time (ms)	1.78 ± 0.05	1.64 ± 0.07	$p = 0.09$
spike halfwidth (ms)	7.39 ± 0.19	7.42 ± 0.33	$p = 0.95$
spike decay τ (ms)	15.23 ± 0.40	12.67 ± 0.50	* $p < 10^{-3}$
PSF amplitude (pA)	6.38 ± 0.56	7.97 ± 0.69	$p = 0.08$
PSF duration (ms)	5.25 ± 0.37	4.81 ± 0.26	$p = 0.34$
PSF area (fC)	16.35 ± 2.28	18.27 ± 1.64	$p = 0.51$

Figures:

Figure 3.1:

a

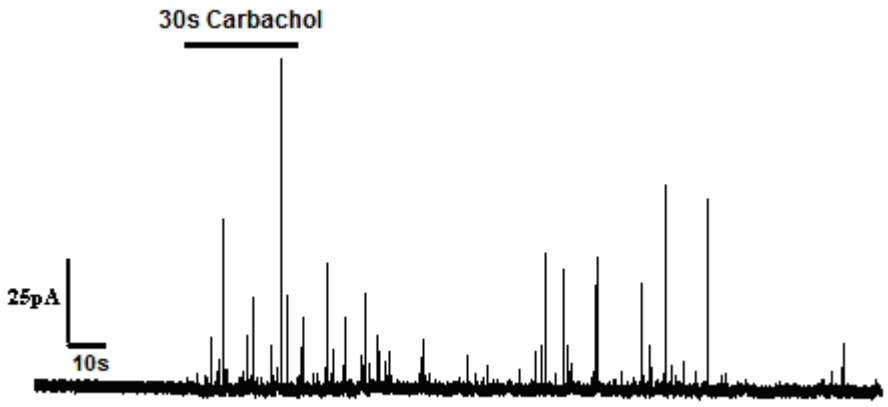

b

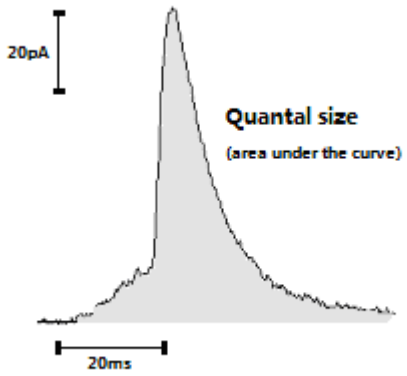

Detection of quantal catecholamine release with carbon fiber electrode amperometry. (a) A typical trace of amperometric recording that showed bursts of amperometric signals when stimulated by a 30 s application of carbachol (1 mM). (b) Sample of an amperometric "spike" signal whose time integral (the area under the curve) was an estimate of the quantal size Q (the amount of catecholamine released from a single granule).

Figure 3.2:

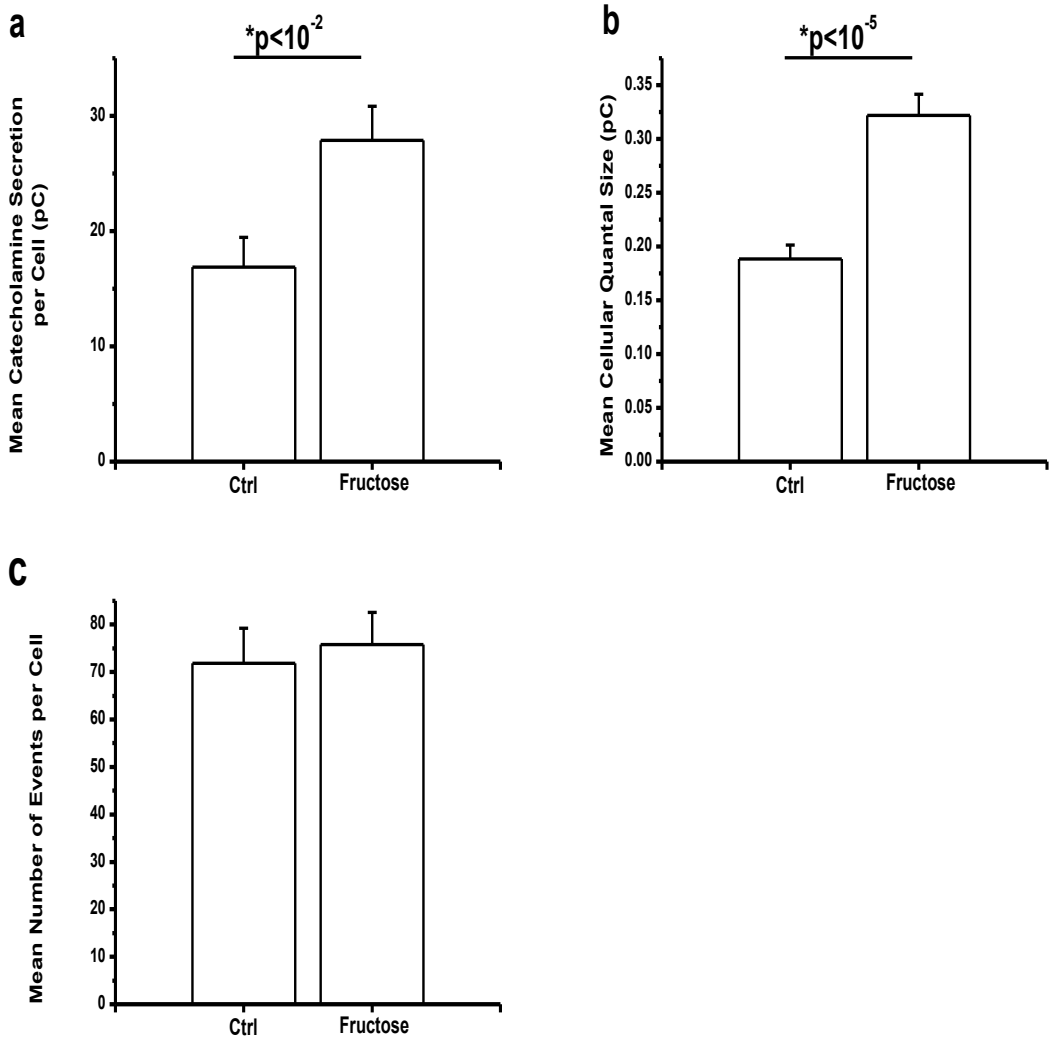

Fructose feeding increased the mean cellular catecholamine secretion and quantal size in chromaffin cells stimulated with 1 mM carbachol. (a) Fructose feeding significantly increased the amount of catecholamine secreted per cell. The total secretion from individual cell was calculated by adding all the areas of individual amperometric signals in the recording trace. (b) The mean cellular quantal size was significantly increased by fructose feeding. (c) Fructose feeding had no effect on the number of spikes per cell evoked by 1 mM carbachol. Data shown was the average of 48 cells from 4 control rats and 62 cells from 5 fructose-fed rats.

Figure 3.3:

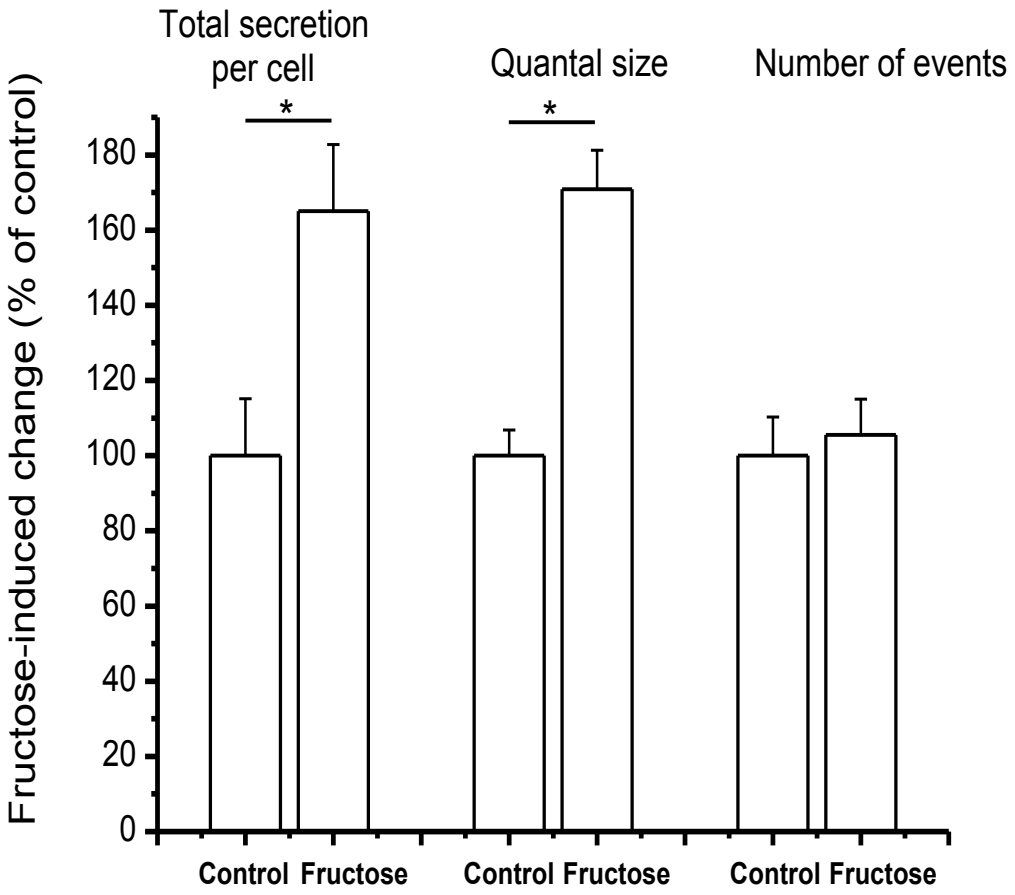

Summary of the fructose-induced changes in catecholamine secretion when cells were stimulated by 1 mM carbachol. The increase in total cellular secretion (~65%) was mainly due to the increase in the quantal size (~70%), rather than a change in the number of secretory granule undergoing exocytosis. Same data set as in Fig. 3.2. Data from the fructose-fed group is normalized to those of the controls.

Figure 3.4

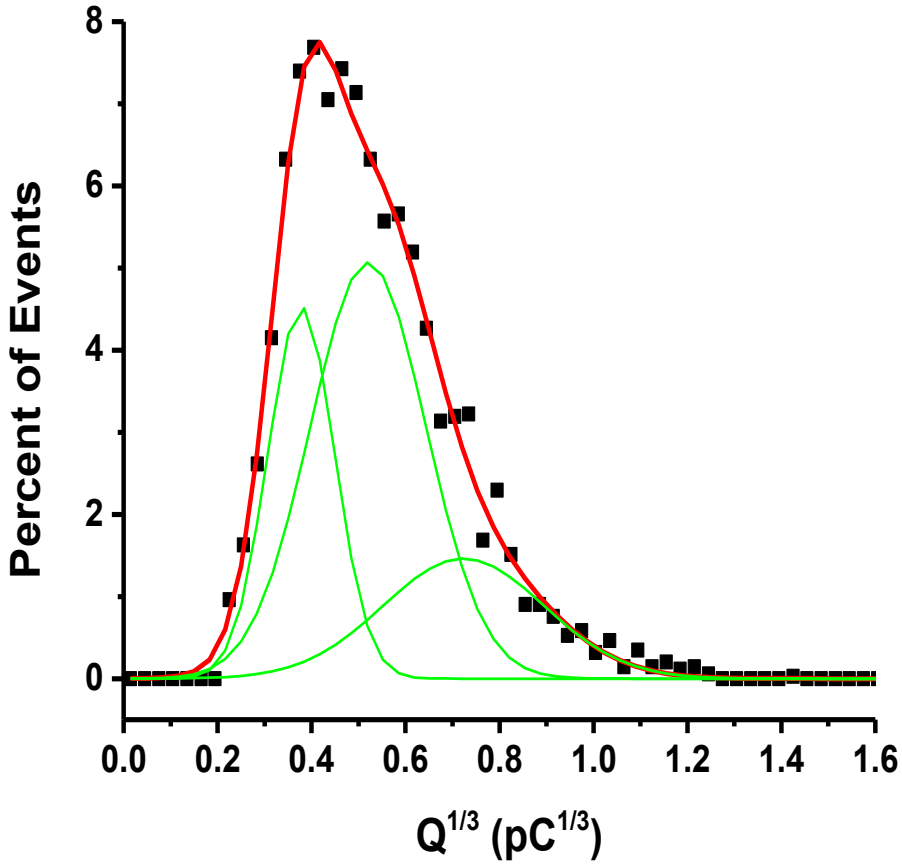

Presence of three populations of granules in chromaffin cells with small, intermediate and large Q values. Plot of the $Q^{1/3}$ distribution of granules exocytosed from cells in the control group when stimulated by 1mM carbachol. The data could be reasonably described by the summation of three Gaussian distributions with peaks located at 0.38 0.52 and 0.72 $pC^{1/3}$.

Figure 3.5:

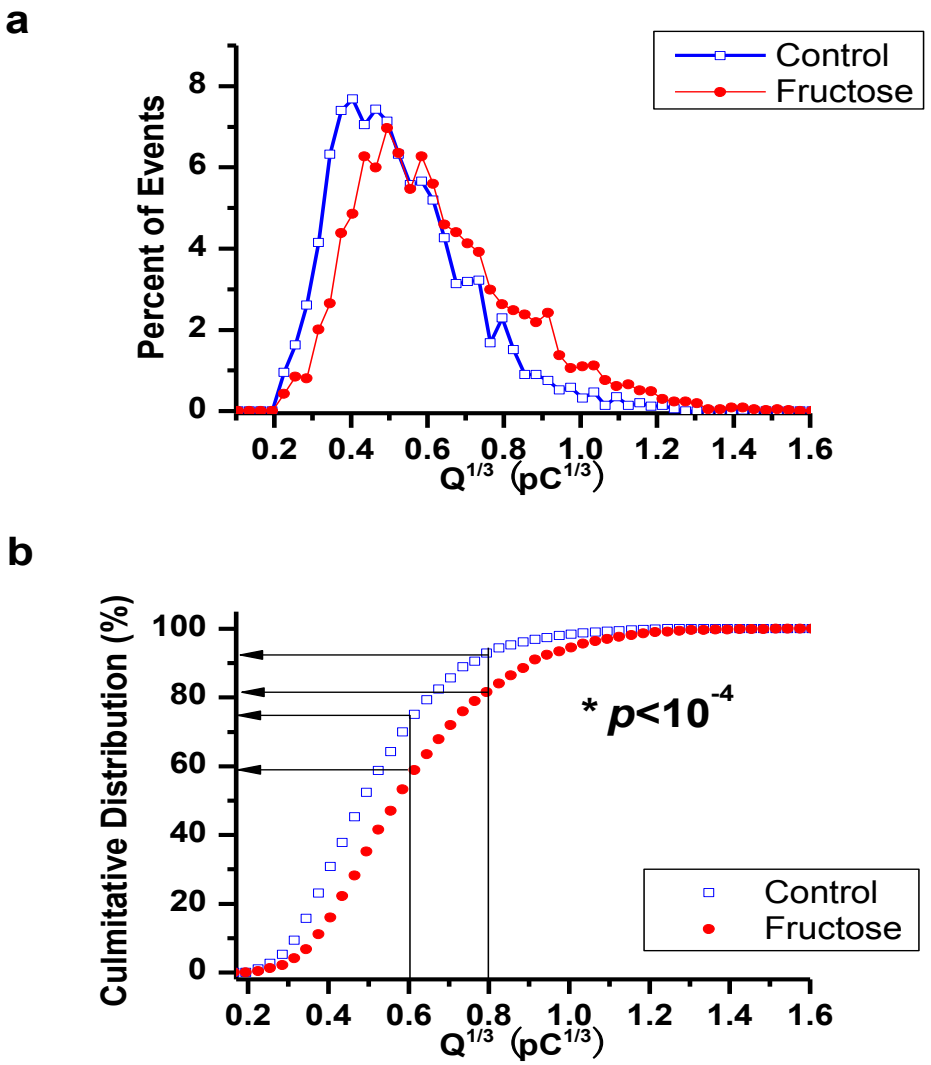

Fructose feeding increased the proportion of intermediate and large Q granules that underwent exocytosis when stimulated by 1 mM carbachol. (a) The $Q^{1/3}$ distribution of granules from the fructose-fed group was right shifted when compared with the controls, indicating that the proportion of granules with a $Q^{1/3}$ value larger than 0.6 $pC^{1/3}$ was increased by fructose feeding. (b) Plots of the cumulative $Q^{1/3}$ distribution of the control and fructose-fed groups. The K-S test indicated a significant difference between the two distributions. Note that the intermediate and large Q granules ($Q^{1/3} \geq 0.6$ $pC^{1/3}$) made up ~25% of the total granules in the control group and this percentage increased to ~40% in the fructose-fed group. In the control group, the large Q granules ($Q^{1/3} \geq 0.8$ $pC^{1/3}$) made up ~8% of total granules and this percentage increased to 20% in the fructose-fed group.

Figure 3.6:

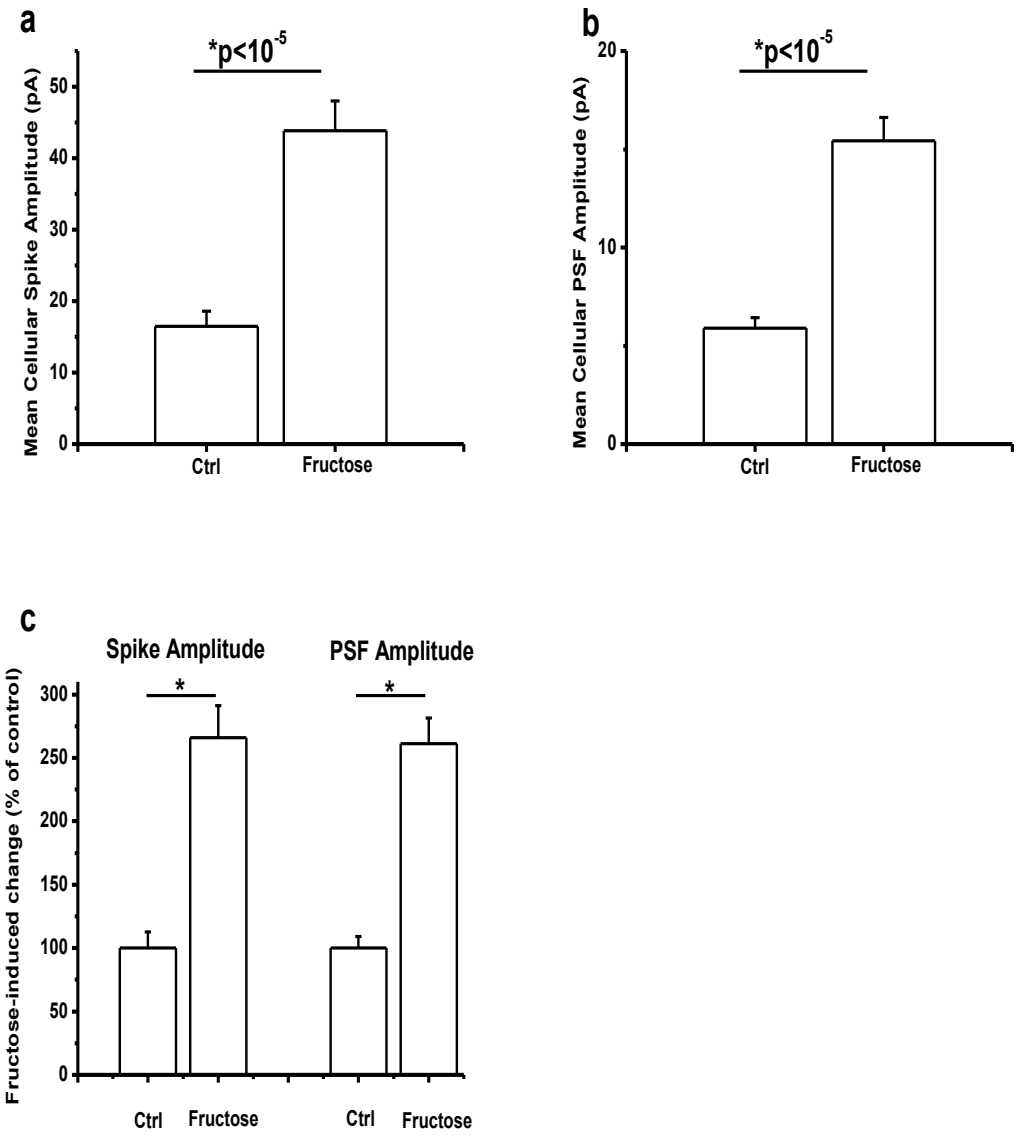

In cells stimulated with carbachol (1 mM), fructose feeding increased the amplitude of the spike signals (a) as well as the prespike foot amplitude (b). (c) Fructose feeding increased the spike and foot amplitudes by the same extent (~ 160%).

Figure 3.7:

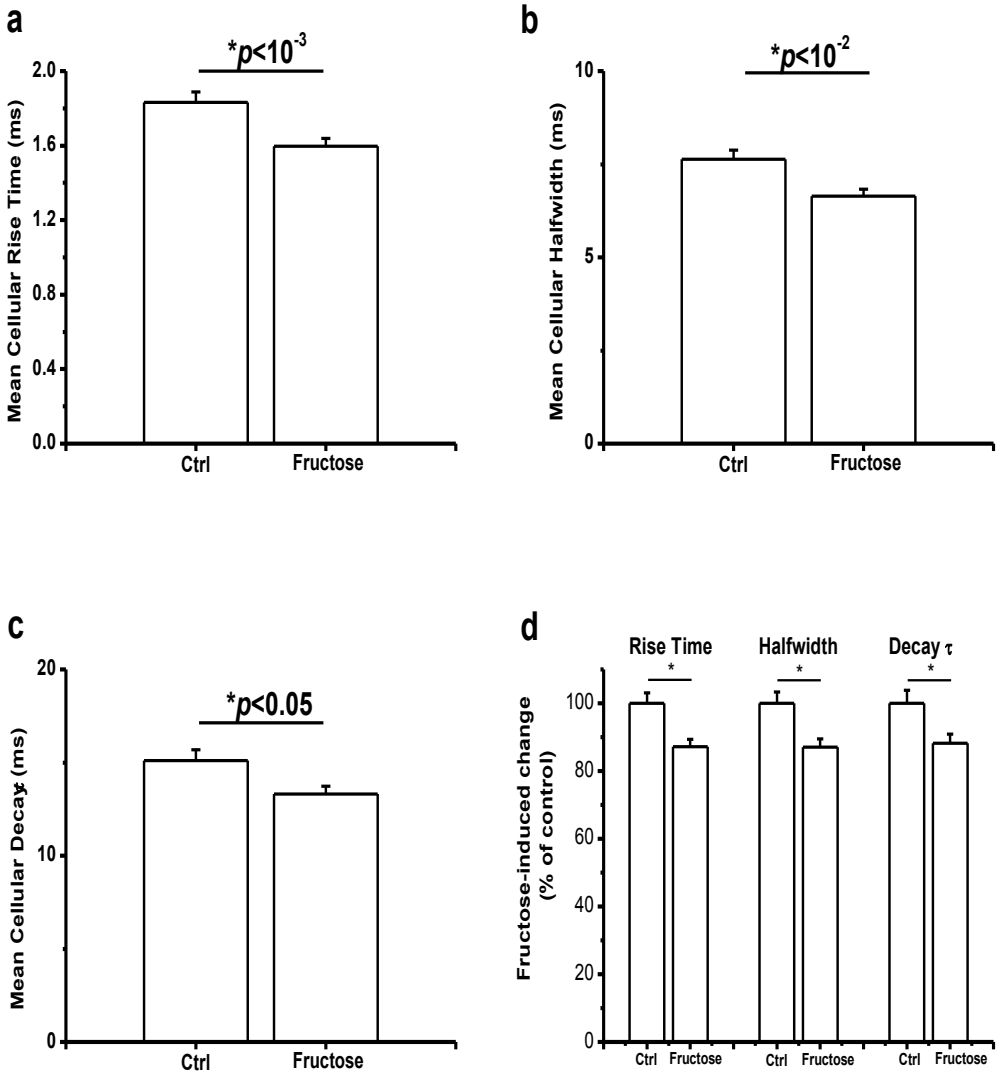

Fructose feeding accelerated the kinetics of the averaged amperometric spike in cells stimulated with 1 mM carbachol. (a) The spike rise time, (b) the halfwidth and (c) the decay τ were decreased significantly by fructose feeding. (d) Fructose accelerated the spike rise time, halfwidth and decay τ to the same extent (by ~14%).

Figure 3.8:

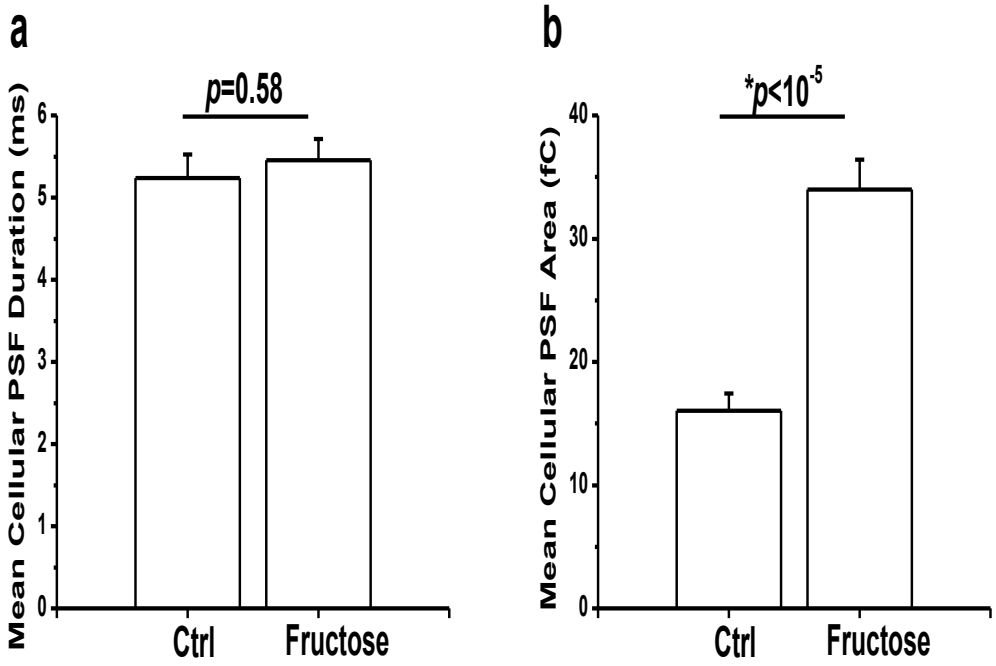

Fructose feeding increased the PSF area of the averaged amperometric spike in cells stimulated with 1 mM carbachol. (a) The average PSF duration was unchanged by fructose feeding. (b) The mean cellular PSF area was increased by ~ 112% with fructose feeding.

Figure 3.9:

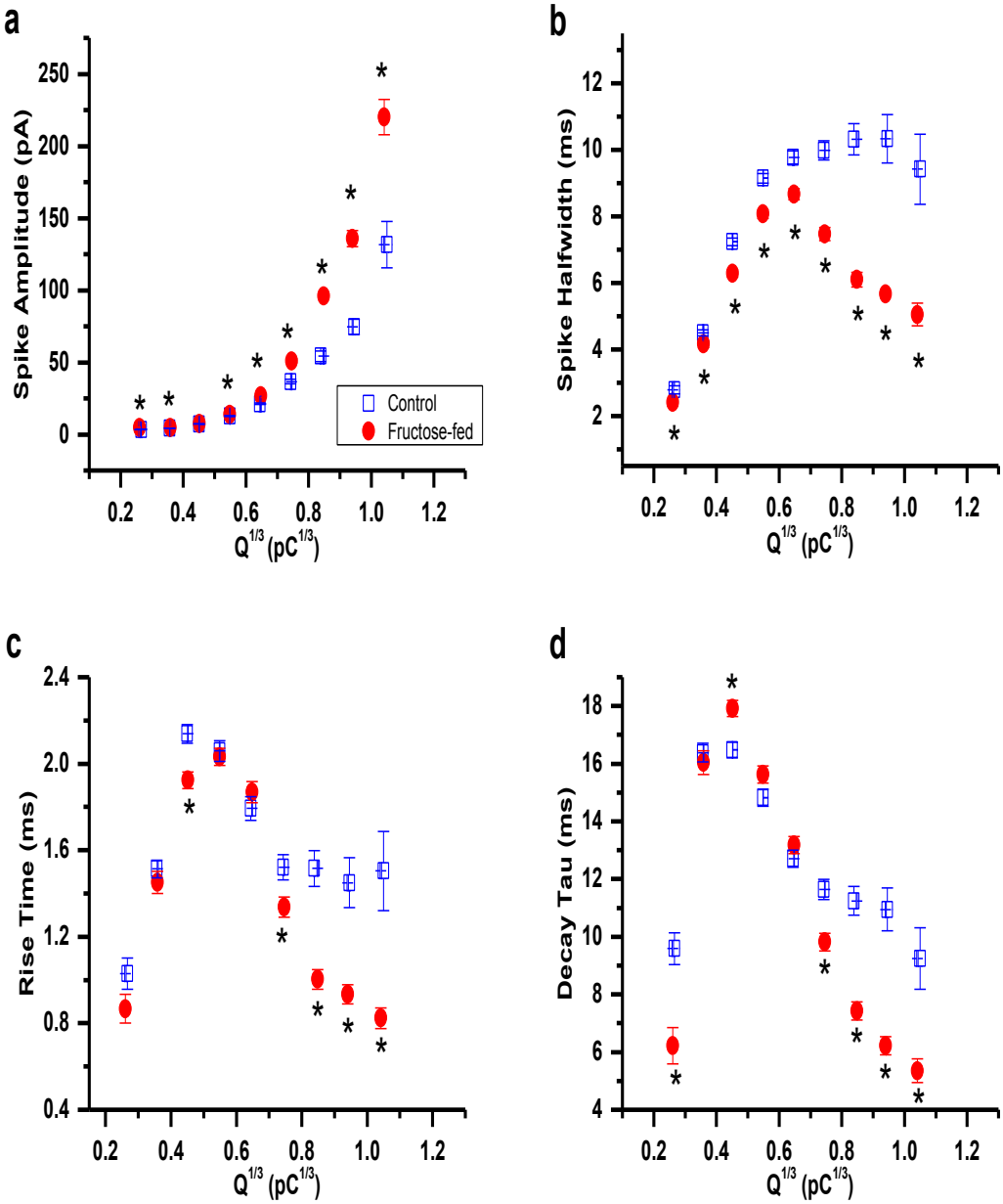

Plots of the the spike kinetics from cells stimulated with carbachol at increasing values of $Q^{1/3}$. Data from the control and fructose-fed groups were compared at matched bin size of 0.1 $pC^{1/3}$. Fructose feeding accelerated the kinetics of amperometric spikes especially in the upper ranges of the $Q^{1/3}$ value (0.65-1.05 $pC^{1/3}$).

Figure 3.10:

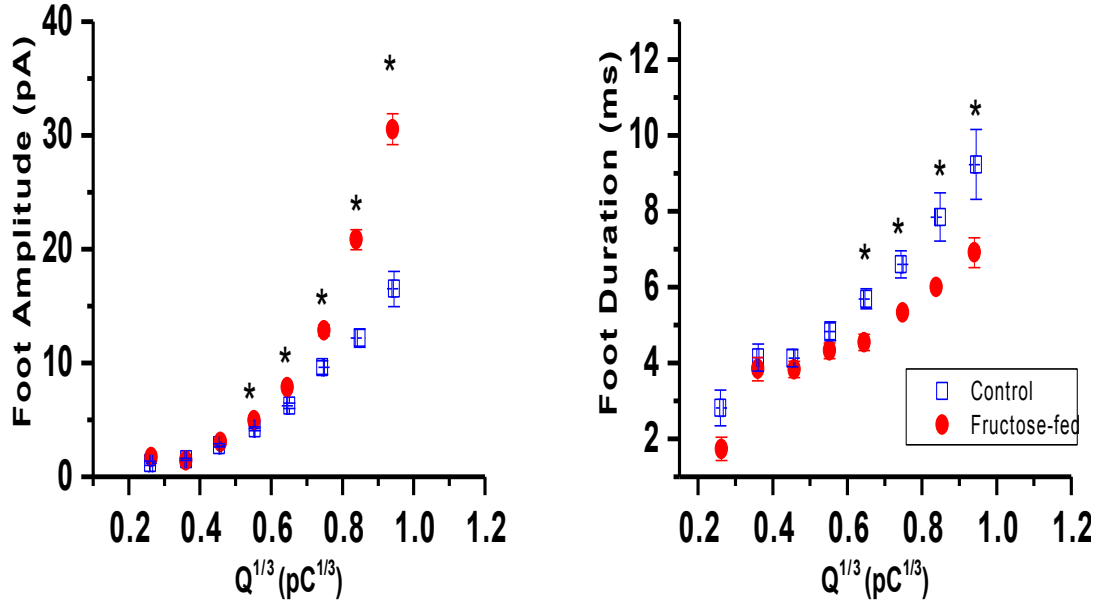

Plots of the the prespike foot (PSF) kinetics from cells stimulated with carbachol at increasing values of $Q^{1/3}$. Data from the control and fructose-fed groups were compared at matched bin size of 0.1 $pC^{1/3}$. Fructose feeding accelerated the kinetics of the PSF signal in the upper ranges of $Q^{1/3}$ value (0.65-1.05 $pC^{1/3}$).

Figure 3.11:

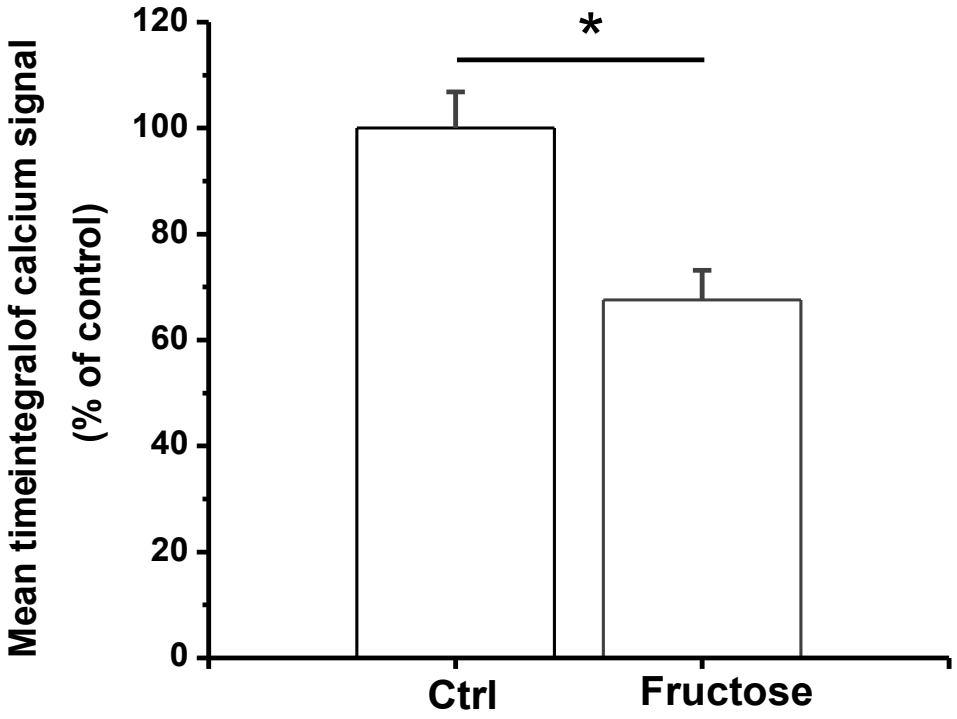

The time integral of the carbachol-evoked Ca^{2+} signal was reduced by fructose feeding. The data from the fructose-fed group was normalized to the controls. Data shown was the average of 26 cells from 1 rat in the control group and 10 cells from 1 rat in the fructose-fed group.

Fig. 3.12

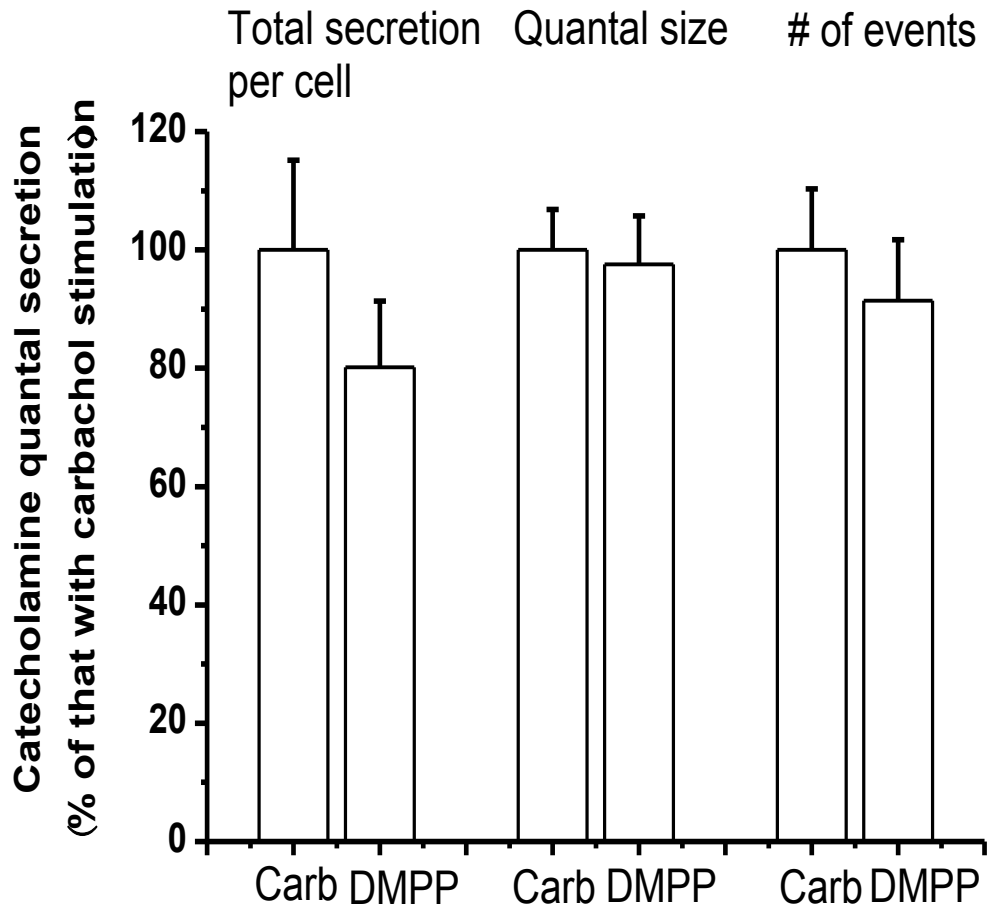

The catecholamine release evoked by DMPP (100 μM) is comparable to that evoked by carbachol (1 mM). In control cells, the average amount of catecholamine secretion per cell, the quantal size and the number of amperometric events evoked by DMPP and carbachol were similar.

Figure 3.13:

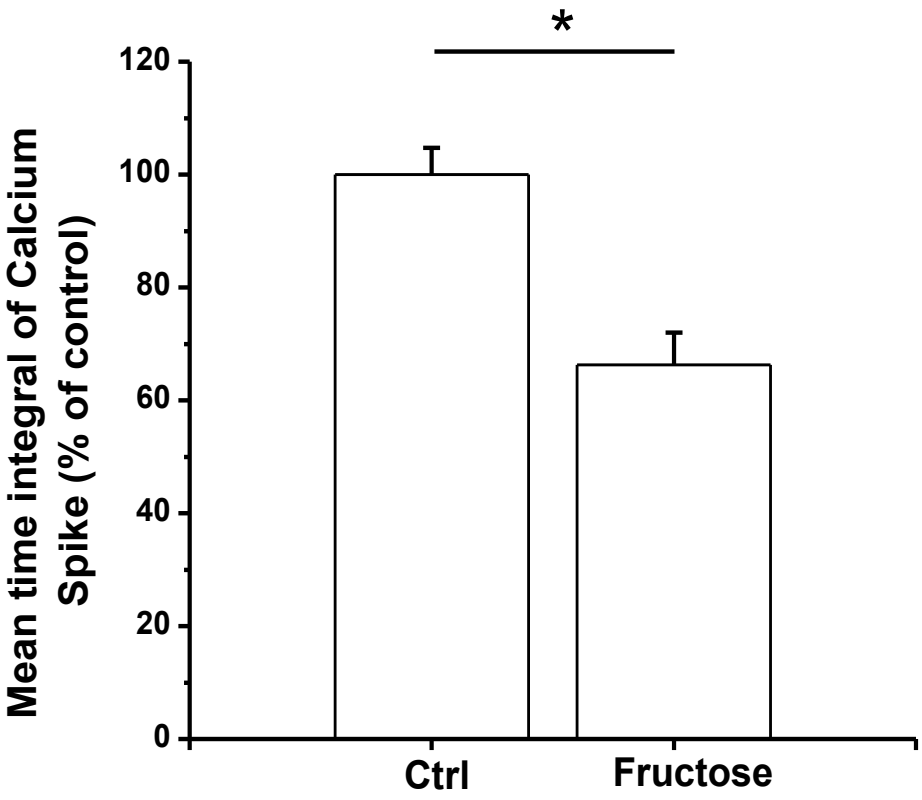

The time integral of the DMPP-evoked Ca^{2+} signal was reduced by fructose feeding. The data from the fructose-fed group was normalized to the controls. Data shown was the average of 39 cells from 1 rat in the control group and 29 cells from 1 rat in the fructose-fed group.

Figure 3.14:

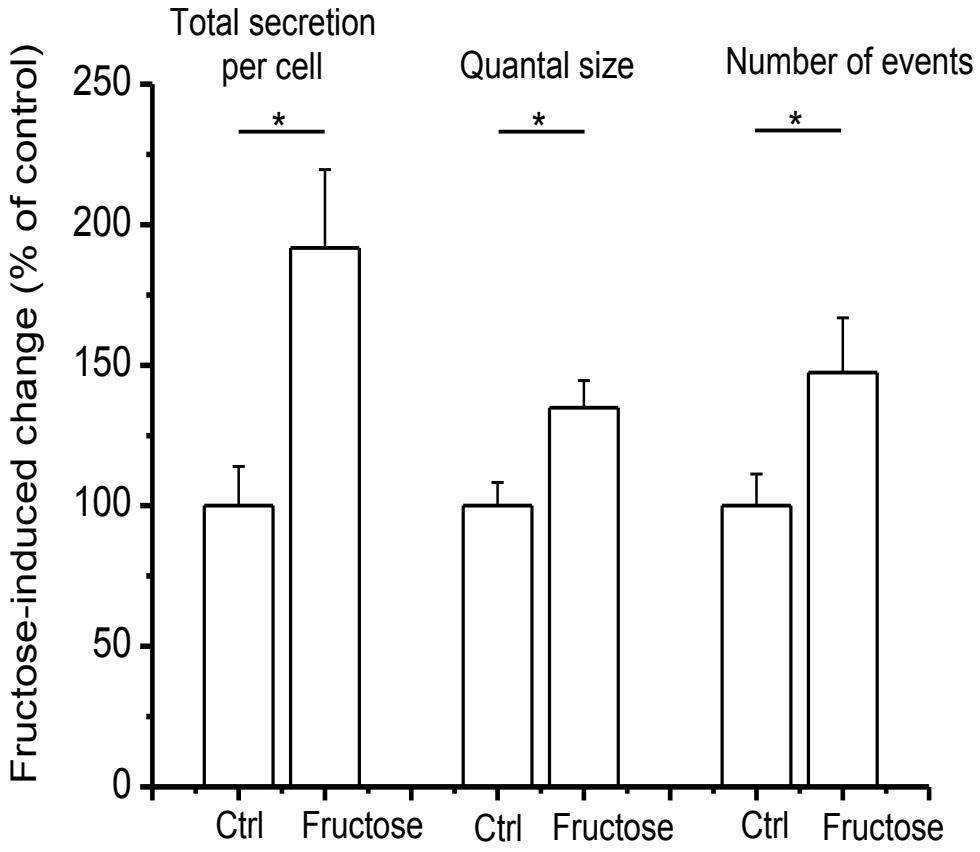

In cells stimulated with DMPP, fructose feeding increased the total secretion from individual cells via an increase in the quantal size and the number of granules. With 100 μM DMPP stimulation, the 92% increase in cellular catecholamine secretion after fructose feeding was associated with a 47% increase in the mean number of amperometric events triggered per cell and a 35% increase in the mean cellular value of Q. Data shown was the average of 49 cells from 3 rats in the control group and 43 cells from 3 rats in the fructose-fed group.

Figure 3.15:

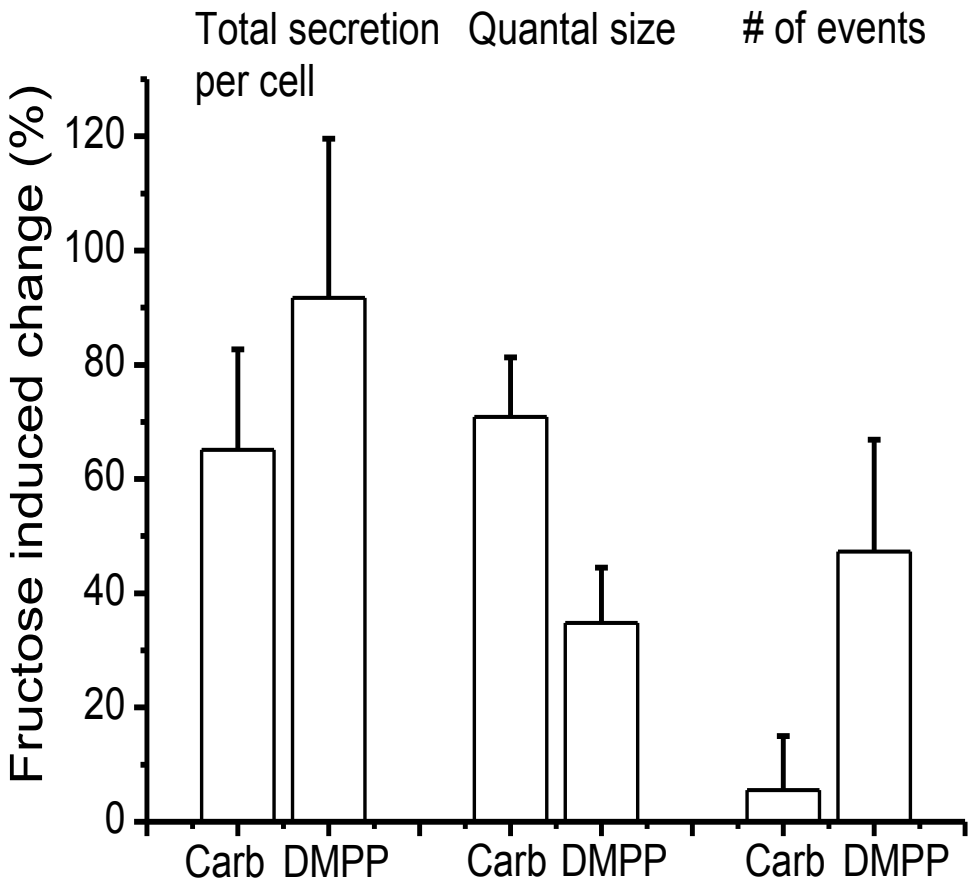

Comparison of the fructose-induced changes in quantal catecholamine release between cells stimulated with carbachol and those stimulated with DMPP. The increase in carbachol-evoked secretion by fructose feeding was mainly due to the increase in quantal size. In contrast, the increase in DMPP-evoked secretion by fructose feeding was related to an increase in the number of granules exocytosed.

Figure 3.16

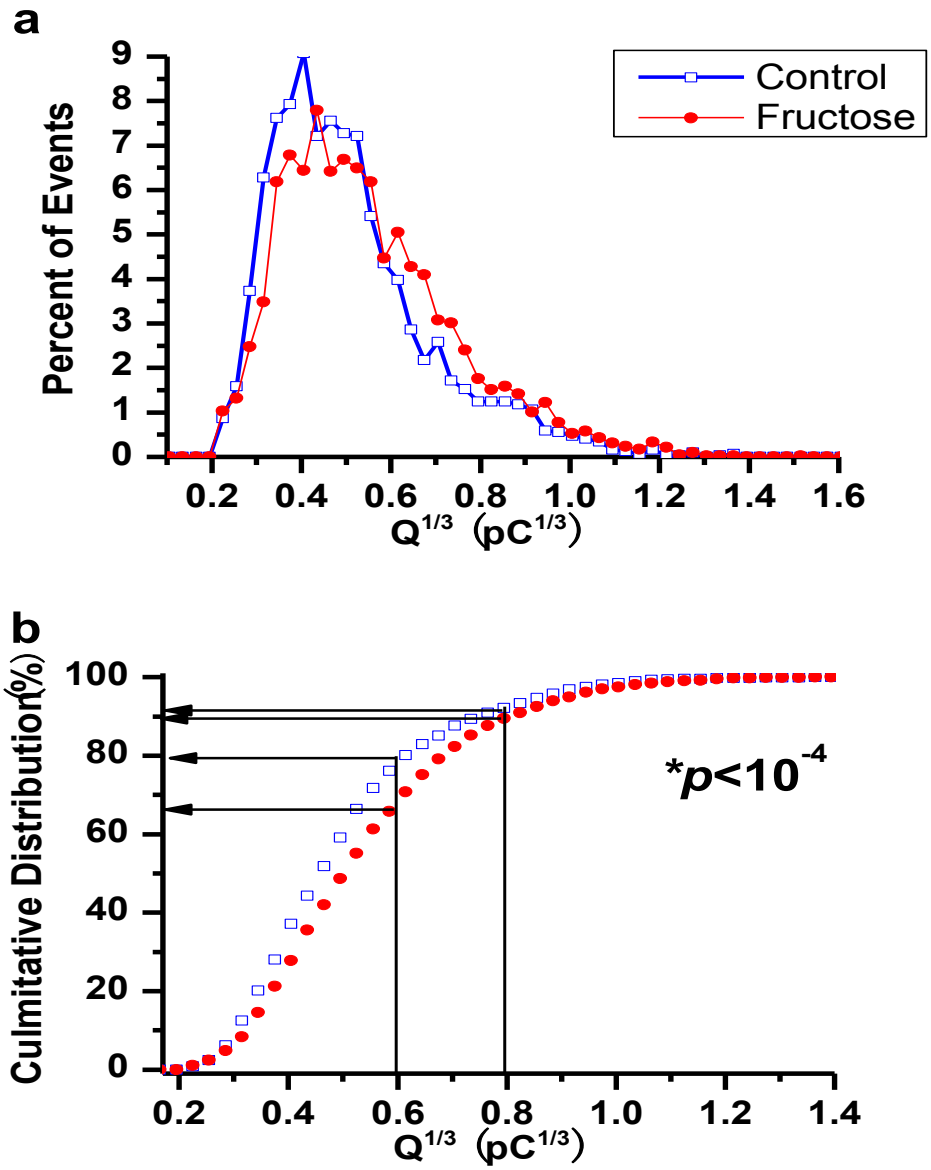

Fructose feeding increased the proportion of intermediate and large Q granules to undergo exocytosis when cells were stimulated by 100 μM DMPP. (a) Fructose feeding caused a small right shift in the $Q^{1/3}$ distribution. (b) The cumulative $Q^{1/3}$ distribution of the fructose-fed data was significantly different from the controls (K-S test). As indicated by the solid lines, granules with a $Q^{1/3} \geq 0.6$ $pC^{1/3}$ comprised ~20% of the total granules triggered in the control group and this percentage increased to ~ 30% in the fructose-fed group. However, for granules with a $Q^{1/3} \geq 0.8$ $pC^{1/3}$, there was little difference between the control and the fructose-fed group.

Figure 3.17:

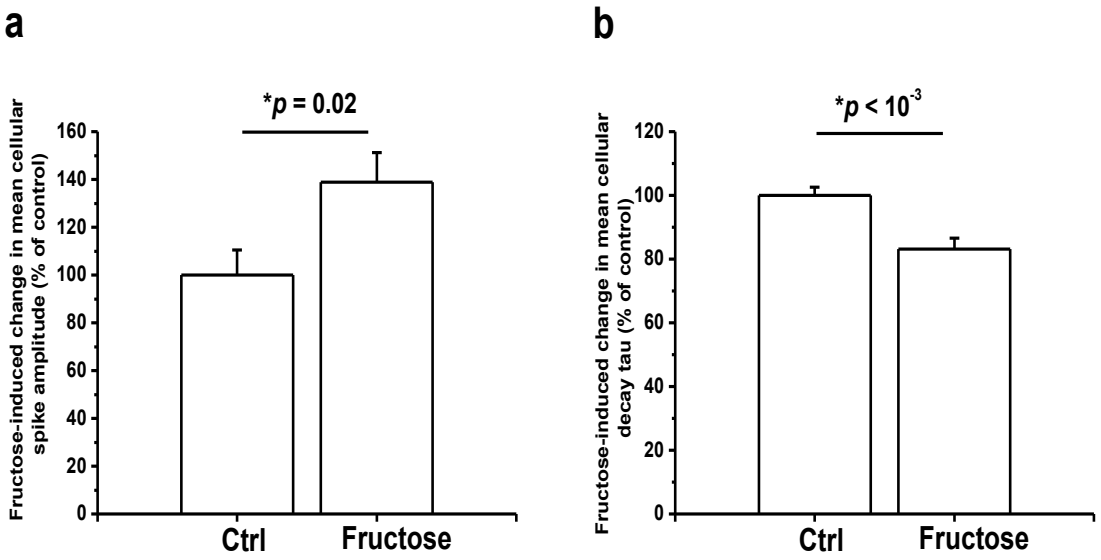

In cells stimulated with DMPP, fructose feeding only increased the spike amplitude and accelerated the spike decay. Comparisons of the cellular mean values of spike amplitude and spike decay τ between the control and fructose-fed group.

Figure 3.18:

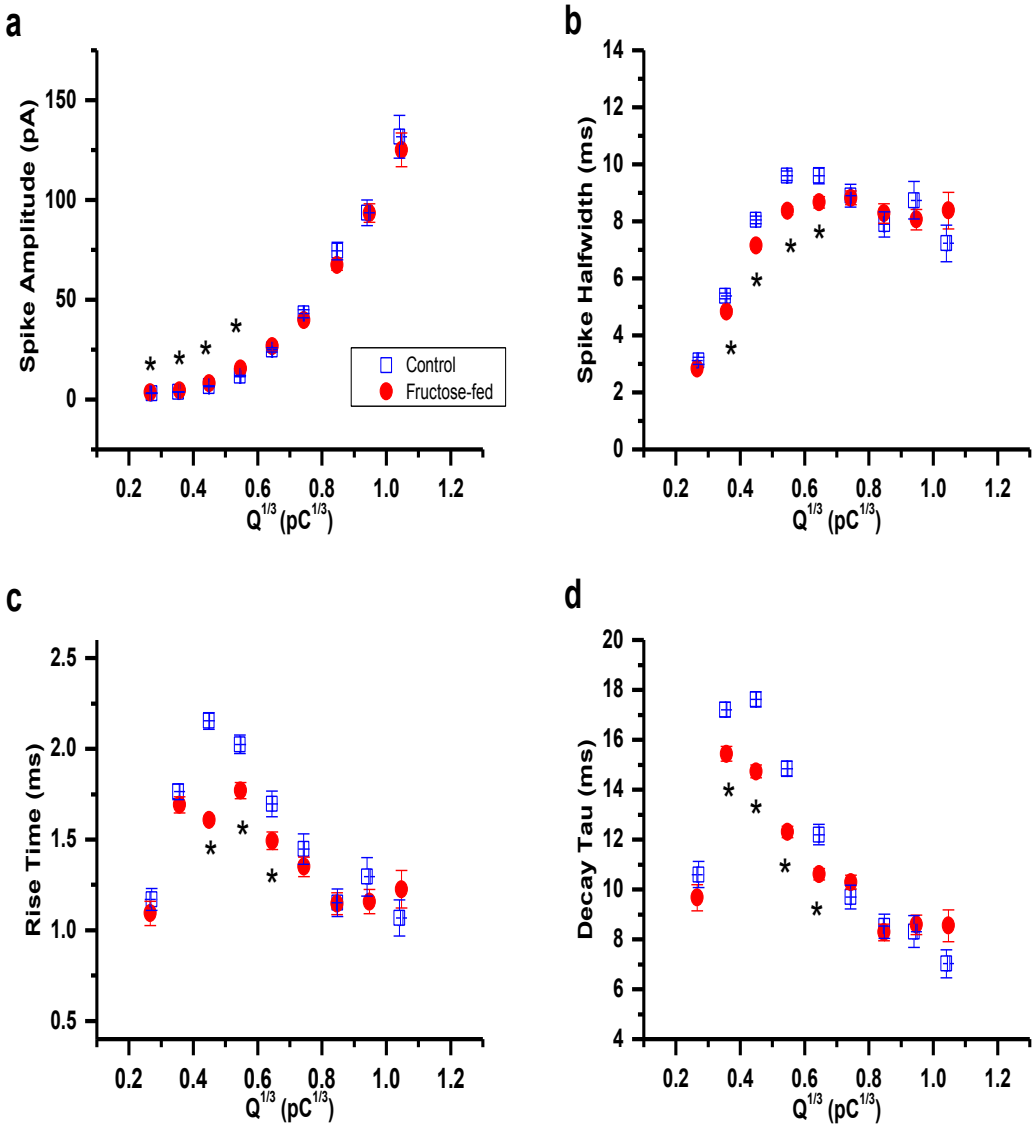

Plots of the spike kinetics from cells stimulated with DMPP at increasing values of $Q^{1/3}$. Data from the control and fructose-fed groups were compared at matched bin size of 0.1 $pC^{1/3}$. Fructose feeding caused only a small but significant increase in the spike amplitude at $Q^{1/3} < 0.6$ $pC^{1/3}$, and selectively shortened the rise time, half width as well as decay τ of the spike at $Q^{1/3}$ between 0.4 and 0.6 $pC^{1/3}$.

Figure 3.19:

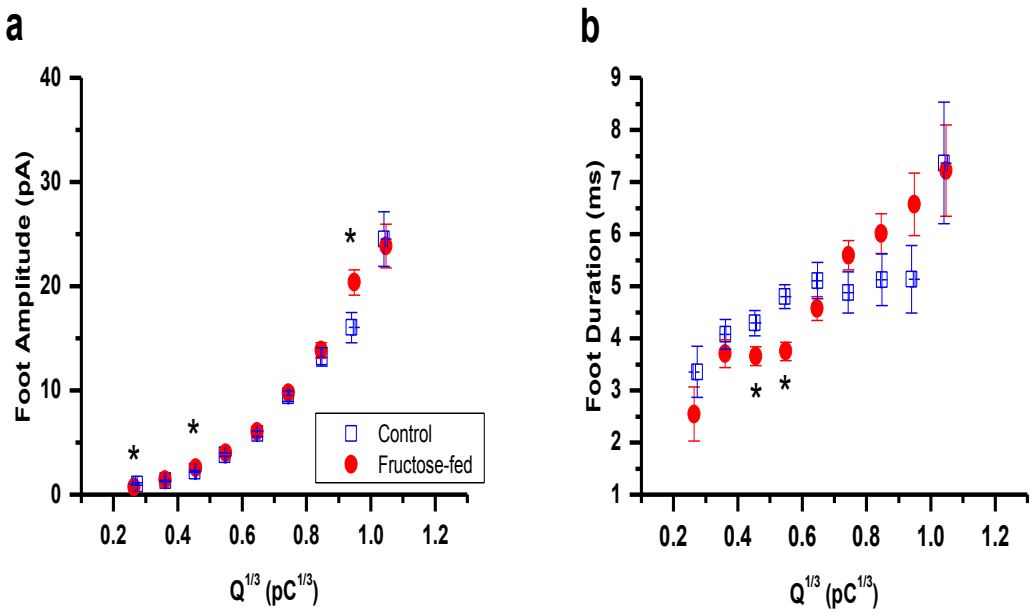

Plots of the the prespike foot (PSF) kinetics from cells stimulated with DMPP at increasing values of $Q^{1/3}$. Data from the control and fructose-fed groups were compared at matched bin size of 0.1 $pC^{1/3}$. Fructose feeding did not accelerate the kinetics of the PSF signal for large Q granules ($Q^{1/3} > 0.6$).

Chapter 4 Discussion:

4.1 *For chromaffin cells stimulated with the nicotinic agonist, DMPP, fructose feeding increased the total catecholamine secretion via an increase in the number of granules, as well as the proportion of intermediate Q granules, to undergo exocytosis*

In chromaffin cells, the nAChRs play a major role in the rapid phase of exocytosis and contribute to the majority of catecholamine secretion under physiologic condition. As shown in Fig. 3.12, the stimulation of chromaffin cells in the control group with 100 μM of DMPP, a selective nicotinic agonist, evoked a similar number of amperometric signals and the amount of catecholamine secretion per cell when compared with cells stimulated with the cholinergic agonist, carbachol (1 mM). Moreover, the mean cellular quantal size was also similar between control cells stimulated with DMPP or carbachol (Fig. 3.12). This finding is consistent with the notion that in control chromaffin cells, nicotinic receptors have a dominant role in the control of quantal catecholamine release.

Fig. 3.14 shows that in cells stimulated with DMPP, fructose feeding induced a large increase (~92%) in the total cellular secretion and this increase was due to the increase in both the number of granule released per cell (increased by ~47%) and the mean cellular quantal size (increased by ~35%). The increase in mean cellular quantal size in the fructose-fed group was due to the release of a larger proportion of granules with an intermediate quantal size. This is supported by the observation that there was a small right-shift of the $Q^{1/3}$ distribution curve of granules from the fructose-fed group when compared with the controls (Fig. 3.16a). Moreover, the cumulative $Q^{1/3}$ distribution in Fig. 3.16b shows that fructose feeding increased the proportion of granules with intermediate Q ($Q^{1/3} \geq 0.6$ $pC^{1/3}$) that underwent exocytosis upon DMPP stimulation by ~10%. In contrast, the proportion of granules with large Q ($Q^{1/3} \geq 0.8$ $pC^{1/3}$) that underwent exocytosis upon DMPP stimulation was not altered by fructose

feeding (Fig. 3.16b). These observations raise the possibility that fructose feeding recruited a population of granules with an intermediate Q, resulting in an increase in the number of granules that underwent exocytosis when stimulated with nicotinic agonist.

In my experiments with DMPP, the cellular mean values of quantal kinetics were not significantly affected in granules from fructose-fed group, except for a 38% taller spike amplitude and a 20% shorter decay τ (Fig. 3.17). When the kinetic parameters of amperometric signals triggered by DMPP were compared at narrow ranges of matched $Q^{1/3}$, fructose feeding did not have any major effect on the kinetics of the foot signal (Fig. 3.19). The spike kinetics of the granules with intermediate or large Q ($Q^{1/3} \geq 0.6$ $pC^{1/3}$) was similar between the fructose and control group (Fig. 3.18). However, for granules with small Q ($Q^{1/3}$ between 0.4 and 0.6 $pC^{1/3}$), fructose feeding caused a small but significant shortening of the rise time, half width as well as decay τ of the spike (Fig. 3.18).

4.2 *For chromaffin cells stimulated with the cholinergic agonist, carbachol, fructose feeding increased total catecholamine secretion via an increase in the proportion of intermediate and large Q granules to undergo exocytosis*

The fructose feeding mediated increase in total cellular catecholamine secretion in the DMPP experiments was also observed when chromaffin cells were stimulated with carbachol (1 mM), a nonselective cholinergic agonist. As shown in Fig. 3.3, in cells stimulated with carbachol, fructose feeding increased the total cellular secretion by ~70%. In contrast to the finding in the DMPP experiment, fructose feeding did not cause any increase in the number of granules released per cell upon carbachol stimulation (Fig. 3.3). However, in cells stimulated with carbachol, the mean cellular quantal size in the fructose-fed group was ~70% larger than the controls (Fig. 3.3). Therefore, in cells stimulated with carbachol, the increase in total secretion per cell by fructose feeding is primarily due to an increase in the mean cellular quantal size.

The large increase in mean cellular quantal size in the fructose-fed group when stimulated by carbachol was associated with a prominent right shift in the $Q^{1/3}$ distribution curve of granules from the fructose-fed group (Fig. 3.5a). Analysis on the cumulative $Q^{1/3}$ distributions in Fig. 3.5b shows that fructose feeding increased the proportion of granules with intermediate Q ($Q^{1/3} \geq 0.6$ $pC^{1/3}$) that underwent exocytosis upon carbachol stimulation by ~15%. Importantly, for granules with large Q ($Q^{1/3} \geq 0.8$ $pC^{1/3}$), the proportion of granules that underwent exocytosis was increased by more than 2-fold after fructose feeding. This finding suggests that in cells stimulated with cholinergic agonist, fructose feeding increased the proportion of both the intermediate and large Q granules to undergo exocytosis.

In the carbachol stimulated cells, the increase in Q after fructose feeding was accompanied by a 2.6-fold increase in the spike and PSF amplitude (Fig. 3.6b). In these cells, fructose feeding also accelerated the spike kinetics; the spike rise time, halfwidth and decay τ were all decreased by ~14% (Fig. 3.7d). Since large Q granules typically have more rapid spike kinetics relative to intermediate Q granules, and fructose feeding caused an increase in the proportion of large Q granules to undergo exocytosis, I examined whether the fructose-induced changes in quantal release kinetics are independent of quantal size by comparing the different kinetic parameters between the control and fructose-fed groups at narrow ranges of matched $Q^{1/3}$ values. As shown by the results in Figs. 3.9 and 3.10, the effects of fructose feeding on release kinetics were independent of quantal size. Interestingly, the effects of fructose feeding on release kinetics were most prominent for the larger Q granules ($Q^{1/3} > \sim 0.7$ $pC^{1/3}$). Fructose feeding not only increased the spike amplitude (Fig. 3.9a) and accelerated the spike kinetics for larger Q granules, but also accelerated the PSF kinetics of these larger Q granules via an increase in the foot amplitude and a shortening of the foot duration (Fig. 3.10). If one assumes that fructose feeding does not change the concentration of catecholamine in the chromaffin granules, then the increase in the amplitudes of the spike and foot signal for the large Q granules

suggests that fructose feeding increases the size of fusion pore before and after its rapid dilation. A bigger fusion pore is expected to accelerate the spike kinetics. Indeed, the spike kinetics of the larger Q granules is also accelerated by fructose feeding; the spike rise time, half-width and decay τ were all shortened by fructose feeding (Fig. 3.9). Therefore, these findings are consistent with the idea that fructose feeding increases the size of the fusion pore. However, the possibility that the granule matrix may de-condense more rapidly after fructose feeding cannot be ruled out.

4.3 *Discrepancy between the effects of fructose feeding on chromaffin cells when stimulated by nicotinic or cholinergic agonist*

The above findings suggested that when mAChRs were co-activated with nAChRs (as with 1 mM carbachol), the augmentation in Q after fructose feeding was larger than that elicited by the selective activation of nAChRs (by DMPP). A parsimonious explanation of the different patterns of the effects of fructose feeding with the two stimuli is depicted in the model shown in Fig. 4.1. In Fig. 4.1, a chromaffin cell with small, intermediate and large diameter granules was depicted to represent the three populations of granules with small, intermediate and large Q. In the control group, stimulation of chromaffin cells by DMPP or carbachol triggered a fraction of small, intermediate and large Q granules to undergo exocytosis. In the fructose-fed group, there was an increase in population of granules with intermediate Q. When cells in the fructose-fed group were stimulated by DMPP, there was an increase in total number of granules underwent exocytosis: especially in the number of granules with intermediate Q. This contrasts with the situation of carbachol stimulation, where the number of granules released was unaltered, but the proportion of intermediate and large Q granules that underwent exocytosis was increased. A possible scenario is that with carbachol stimulation, the activation of muscarinic receptors evoked the release of Ca^{2+} from intracellular stores and the rise in $[Ca^{2+}]_i$ promoted some granules to undergo some form of granule-granule fusion before exocytosis (Cochilla et al., 2000;Machado et al., 2001). As a result, there was an

increase in the proportion of large Q granules that underwent exocytosis upon carbachol stimulation. Consistent with the notion that muscarinic receptor stimulation may promote granule-granule fusion, a study on rat pancreatic β cells has found that the activation of muscarinic receptors during glucose stimulation triggers granule-granule fusion (or compound exocytosis) which contributed to 15-20% of the total fusion events (Hoppa et al., 2012). We speculate that some of these large Q granules generated from granule-granule fusion may have more rapid kinetics. There can be at least two reasons for their faster release kinetics. Firstly, the pre-fused granules can have their surface area to volume ratio changed, which may increase the driving force for fusion pore dilation and/or decondensation of the granule matrix, and thus accelerates the release kinetics. Secondly, the pre-fused granules may have extra copies of the fusion machinery, resulting in a bigger fusion pore and thus have faster release kinetics.

Another mechanism that may contribute to the increase of quantal size associated with mAChRs and nAChRs co-activation in the fructose-fed rat chromaffin cells is protein kinase C (PKC). The activation of PKC as a consequence of mAChRs (M1, M3, M5 subtypes) stimulation and the phospholipase C signaling pathway, has been shown to increase quantal size and overall catecholamine secretion in chromaffin cells (Chen et al., 2005;Currie, 2010). The enhancing effect of PKC involves the abolishment of the feedback inhibition on catecholamine secretion mediated by ATP and μ-opioids which are co-released with catecholamines. The feedback inhibition by ATP and μ-opioids is achieved through their selective activation of a $G_{i/o}$ pathway and its $G_{\beta\gamma}$ subunit. The $G_{\beta\gamma}$ subunit inhibits secretion by reducing the open time of the fusion pore via a mechanism that may involve the alteration of dynamin, the protein responsible for fission of endocytotic vesicles and closure of fusion pore (Chen et al., 2005). PKC activation was found to oppose the action of ATP on the fusion pore (Chen et al., 2005). According to this scenario, an up-regulation of any of the mAChRs subtypes that activates PKC can contribute to the bigger quantal size of granules from the fructose-fed rat chromaffin cells. There is evidence that rat

chromaffin cells express M3 and M4 receptors (Barbara et al., 1998) and the M4 activates $G_{i/o}$ signaling pathway. Therefore, the ratio of active M3 to M4 mAChRs may have a significant impact on quantal size when chromaffin cells are stimulated with a cholinergic agonist (Barbara et al., 1998).

Consistent with an important role of muscarinic receptors stimulation in the regulation of quantal size and release kinetics, amperometric signals with larger Q and faster kinetics were indeed associated with mAChRs activation. When control cells were stimulated with 100 μM muscarine or carbachol (which activates mAChRs either exclusively or more selectively), the quantal size of granules was significantly larger when compared to cells stimulated with 1 mM carbachol, which stimulates the nAChR component more robustly. Moreover, when amperometric signals from control cells were compared, stimulation with 100 μM muscarine significantly accelerated the spike kinetics parameters and tended to have a larger quantal size relative to those stimulated by 100 μM DMPP (Appendix, Table 4).

4.4 *The discrepancy between the direction of changes in Ca^{2+} signal and catecholamine secretion after fructose-feeding*

When compared with the control group, the mean time integral of $[Ca^{2+}]_i$ signal in the chromaffin cells from fructose-fed rats was decreased by ~30% when stimulated by 100 μM DMPP or 1 mM carbachol even though the total secretion per cell was increased by ~70-90%. In addition, when chromaffin cells were stimulated by 100 μM carbachol where the mean time integral of $[Ca^{2+}]_i$ spike was significantly smaller than that with 100 μM DMPP or 1 mM carbachol, there was still a ~30% decrease associated with fructose feeding (Fig. 1 in Appendix). My preliminary data from western blot experiment indicated that there might be a down regulation of the expression of nAChRα-3 and nAChRα-7 (the two more abundant nAChRs subtypes) in the fructose-fed rat chromaffin cell membrane (data not shown). Such a down-regulation of the nAChRs may limit the $[Ca^{2+}]_i$ rise by restricting the

depolarization triggered by nicotinic receptor stimulation. Thus, a down-regulation of nAChRs in fructose-fed rat chromaffin cells may contribute to the reduction of the Ca^{2+} signal evoked by DMPP or carbachol.

A former graduate student in my lab, Michael Simpson, found that the same protocol of fructose feeding affected neither the peak nor the plateau amplitude of the $[Ca^{2+}]_i$ rise triggered by elevating extracellular $[K^+]$ to 50 mM for 5 mins, suggesting that activation of VGCC was not affected by fructose feeding. However, it remains possible that fructose feeding may induce subtle changes in the expression of different types of VGCC in rat chromaffin cells. Rat chromaffin cells express Ca_v1 (L-type) and Ca_v2 (N-, P/Q-, and R-types) VGCCs and these subtypes of VGCC contribute differently to catecholamine secretion (Novara et al., 2004).

While the overall Ca^{2+} signal evoked by DMPP or carbachol was reduced, it remains possible that an increase in the expression of specific types of VGCC by fructose feeding may contribute to an increase in catecholamine secretion. More recently, stress was found to cause an up-regulation of the normally weakly expressed Ca_v3 or T-type VGCC in chromaffin cells, resulting in an increase in stimulation-secretion coupling efficiency (Novara et al., 2004;Guerineau et al., 2012). In stressed rats, an increase in the density of T-type VGCC was postulated to contribute to an increase in spontaneously firing in chromaffin cells in the adrenal gland slices (Colomer et al., 2008). In response to chronic β-adrenergic activation or stress such as hypoxia, the Ca_v3 channels in rat chromaffin cells were recruited via the cAMP-receptor protein Epac ((cAMP-guanine nucleotide exchange factor) cAMP-GEF) signaling pathway (Novara et al., 2004;Carabelli et al., 2007;Giancippoli et al., 2006). Since autocrine activation of β-adrenergic receptors on rat chromaffin cells can occur under basal catecholamine secretion, an augmentation of basal catecholamine secretion by fructose feeding can increase the recruitment of Ca_v3 channels and thus increase stimulation-secretion coupling (Novara et al., 2004). In addition, the signaling pathway recruited by β-adrenergic receptor stimulation

crosstalks to the ones induced by chronic/intermittent hypoxia including the reactive oxygen species (ROS)-dependent Ca^{2+} signaling pathway, leading to the incorporation of Cav3.2 channels during stressor stimulation (Guerineau et al., 2012;Novara et al., 2004;Yuan et al., 2008). Interestingly, the increased ROS production was also associated with fructose feeding and may underlie the pathogenesis of fructose-fed rats (Tran et al., 2009). Therefore, future studies may need to examine whether fructose feeding affects the expression of specific types of VGCCs.

On the other hand, it is possible that a decrease in nAChRs in chromaffin cells of the fructose-fed rats is accompanied by an increase in mAChRs. Since the Ca^{2+}-signal evoked by mAChR stimulation has a small contribution to the overall $[Ca^{2+}]_i$ rise induced by cholinergic stimulation, an increase in mAChRs has little impact on the carbachol-induced Ca^{2+} signal. However, as described above, the intracellular Ca^{2+} release and/or PKC activation triggered by muscarinic receptor stimulation can augment quantal catecholamine release by promoting granule-granule fusion or by opposing the inhibitory action of ATP on the fusion pore. This scenario may explain the discrepancy between the decrease in evoked-Ca^{2+} signal and the increase in catecholamine secretion.

In summary, when the mAChRs in the fructose-fed rat chromaffin cells were co-stimulated with nAChRs robustly by 1 mM carbachol, the overall secretion of catecholamine was increased significantly. This increase is mainly due to the secretion of granules that had a larger quantal size and faster kinetics in quantal catecholamine release. Fructose feeding increased catecholamine release with a different pattern when nAChRs are selectively stimulated; the increase in quantal size was smaller but a larger number of granules underwent exocytosis. The different patterns suggested that after fructose feeding a larger proportion of granules with larger Qs, which were only triggered by 1 mM carbachol, might arise from granule-granule fusion that involved the activation of mAChRs. In addition, such granules may have larger fusion pores during exocytosis that contribute to their more rapid kinetics in quantal release

of catecholamine.

My results indicate that a high fructose diet directly up-regulates the release of catecholamines from adrenal medullary chromaffin cells, which can significantly contribute to the development or maintenance of hypertension. Further investigations on the mechanisms that cause the increase of catecholamine release from fructose-fed rats will be essential for the discovery of cellular targets that are relevant to the pathogenesis of hypertension.

Figures:

Figure 4.1:

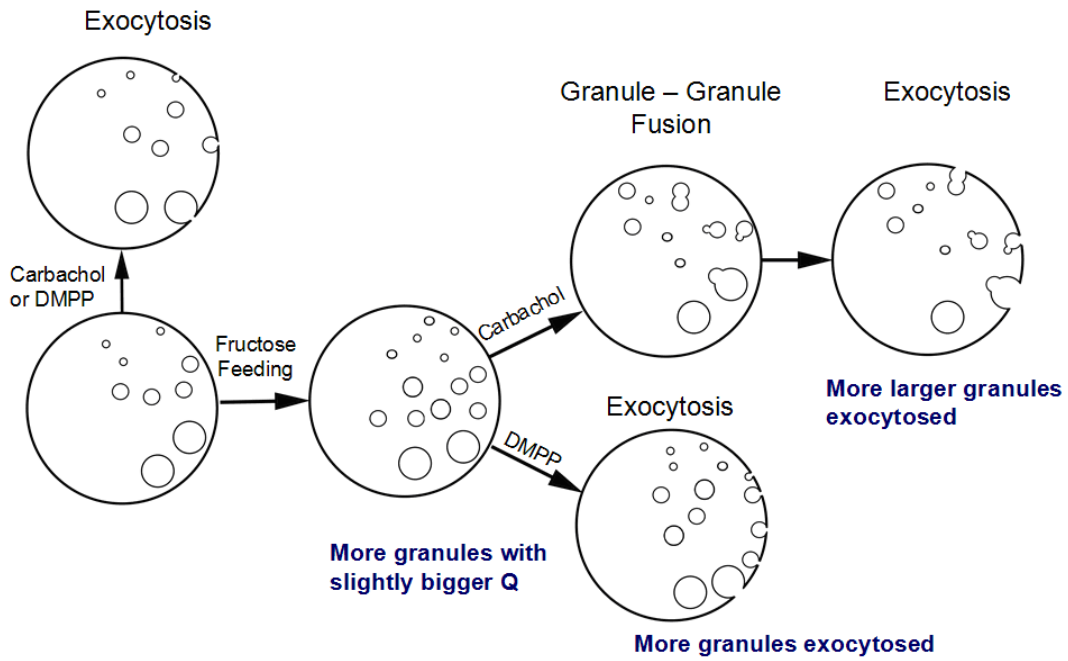

A model that depicts the changes in quantal catecholamine release induced by fructose feeding upon selective activation of nAChR or co-activation of nAChR and mAChR in chromaffin cells.

Appendix:

This chapter documents the amperometry experiments in which chromaffin cells were stimulated with 100 μM carbachol or muscarine. Such experiments were designed to test whether effects of fructose feeding on quantal catecholamine secretion are attributable to an altered expression or signaling of mAChRs. The concentration of 100 μM carbachol or muscarine was chosen because while both stimuli were expected to activate mAChRs robustly, 100 μM carbachol was expected to also activate nAChR significantly (Shirvan et al., 1991).

In control cells, the peak rise in $[Ca^{2+}]$ triggered by 100 μM carbachol was only 72% of that triggered by 1 mM carbachol (403.7 ± 19.2 nM vs 557.8 ± 29.4 nM; $p = 3 \times 10^{-5}$); while the mean time integral of the $[Ca^{2+}]_i$ rise triggered by 100 μM was only 43% of that triggered by 1 mM carbachol (19.67 ± 1.37 μM.s vs 45.69 ± 3.11 μM.s; $p < 10^{-5}$). When 100 μM carbachol was the stimulus, fructose feeding reduced the peak rise in $[Ca^{2+}]$ by 14% (to 347.9 ± 21.6 nM; $p = 0.069$) and the mean time integral of the $[Ca^{2+}]_i$ rise by 27% (to 12.49 ± 0.95 mMs; $p = 5 \times 10^{-4}$) (Fig. I).

Fructose feeding also lowered the fraction of cells that responded to the 100 μM carbachol stimulus with amperometric signals. When stimulated with 100 μM carbachol, 73.87 ± 6.17% of cells (55 out of 72 cells) from the control group responded with more than 1 amperometric spike but only 43.02 ± 5.15% (34 out of 72 cells) responded with more than 10 spikes. When the same criteria were applied to the fructose-fed group, the fraction of cells responded was lower; 54.93 ± 5.90% (47 out of 86 cells) exhibited more than 1 amperometric spike and only 39.54 ± 7.25% (34 out of 86 cells) exhibited more than 10 amperometric spikes.

When control cells that responded to 100 μM carbachol with at least 10 amperometric signals were further analyzed (see Table Ⅰ), their total amount of

catecholamine secretion per cell was comparable to that recorded from control cells stimulated with 1 mM carbachol (15.28 ± 3.57 pC by 100 μM vs 16.88 ± 2.55 pC by 1 mM and; p = 0.71). The lower concentration of catecholamine stimulated ~41% fewer amperometric signals per cell (42.9 ± 7.2 vs 71.8 ± 7.4; $p = 0.6 \times 10^{-3}$), but increased the mean cellular quantal size by ~37% (0.26 ± 0.02 pC vs 0.19 ± 0.01 pC; $p<10^{-2}$; Fig. II). The larger quantal size stimulated by the lower concentration of carbachol was accompanied by a bigger amplitude of the spike and PSF, as well as the area of the PSF (see Table Ⅰ) while kinetic parameters of the amperometric signal were not significantly changed. The overall findings summarized above raised the possibility that when mAChRs were significantly stimulated, a more robust co-stimulation of nACh receptors paradoxically reduces the mean quantal size.

As summarized in Table Ⅱ and Fig. Ⅱ, when cells were stimulated with 100 μM carbachol, fructose-feeding caused no significant effect on the total secretion per cell, the number of amperometric events triggered per cell, or the cellular quantal size. The above pattern contrasts with the observations reported in Chapter 3, that fructose feeding robustly enhanced the secretion of catecholamine per cell and the quantal size by similar proportion when the stimulus was 1 mM carbachol. When other kinetics parameters of amperometric signals stimulated with 100 μM carbachol from control and fructose-fed cells were compared, fructose feeding resulted in a significantly shorter halfwidth and larger PSF amplitude (Table Ⅱ). These changes were in the same direction as those observed in cells from the fructose-fed group when stimulated with 1 mM carbachol.

When 100 μM muscarine, the selectively mAChRs agonist, was the stimulus, 56% of the control cells (n = 35 cells from 2 rats) responded with more than 1 spike, while 33% responded with more than 10 spikes. With fructose feeding (n = 9 cells from 1 rat), the corresponding response rates were 67% and 33% respectively. Since the data for fructose group was from a very small sample, I focused on analyzing the effects of muscarine stimulation within the control group.

In control cells, the peak rise in $[Ca^{2+}]_i$ triggered by 100 μM muscarine was only 153.9 ± 10.0 nM while the mean time integral of the $[Ca^{2+}]_i$ rise was 8.94 ± 0.88 μM.s (Fig. III). The $[Ca^{2+}]_i$ rise stimulated by 100 μM muscarine was significantly lower than that evoked by all the other tested agonists, including 100 μM carbachol. This probably explained the low percentage of cells responded to muscarine. Interestingly, studies on chromaffin cells have suggested that $[Ca^{2+}]_i > 300$ nM is required to trigger exocytosis in chromaffin cells (Burgoyne and Morgan, 1995).

As summarized in Table Ⅲ, among control cells that responded with at least 10 amperometric signals, 100 μM muscarine triggered only ~51% of the amount of secretion per cell when compared with 100 μM carbachol (7.86 ± 1.50 pC with muscarine, 15.28 ± 3.57 pC with carbachol, $p = 0.23$; Table Ⅲ). The number of amperometric signals triggered per cell and the mean cellular value of Q stimulated by 100 μM muscarine also tended to be marginally lower than that stimulated with 100 μM carbachol. In general, the kinetic parameters of the amperometric signals triggered by 100 μM muscarine or carbachol were very similar; the only exception was that the spike halfwidth was 22% smaller when muscarine was the stimulus (Table Ⅲ).

To examine if the mAChR activation and nAChR activation lead to different patterns of quantal catecholamine secretion, the amperometric data were compared between 100 μM muscarine and DMPP stimulation (Table IV). For the same reason addressed above, I only compared the control cells. However, even for these two larger samples of cells, I must emphasize that the analysis in Table IV excluded 12% of the cells which responded poorly to DMPP (i.e. with < 10 amperometric signals), but over 2/3 of the cells which responded poorly to muscarine. The exclusion of a much larger proportion of cells responding poorly to muscarine is expected to overestimate grossly the total secretion per cell with this stimulus. Nevertheless, even with such a bias in our analysis, the total secretion of catecholamine per cell and the

number of amperometric signals triggered by muscarine were only ~58% (p = 0.15) and 54% (p = 0.06) of that triggered by DMPP. The quantal size of amperometric spikes stimulated by 100 μM muscarine seemed to ~27% larger than those stimulated by the 100 μM DMPP (0.23 ± 0.03 pC with muscarine versus 0.18 ± 0.02 pA with carbachol, p = 0.14). The spike amplitude, PSF amplitude and PSF charge were all significantly increased (by 81%, 82% and 72% respectively), while the spike halfwidth shortened (by 22%), when muscarine was the stimulus. The data in Table IV suggests that the amperometric signals triggered by selective activation of mAChR, in comparison to those triggered by nAChR, are fewer in numbers, have larger quantal size and more rapid spike kinetics.

Tables:

Table I:

Comparisons of the amperometric experimental results from control chromaffin cells with 100 μM or 1 mM carbachol stimulation. The data from 100 μM carbachol stimulation was averaged from 34 cells obtained from 5 rats, and the data from 1 mM carbachol stimulation was averaged from 48 cells obtained from 4 animals.

Control	100 μM carbachol	1 mM carbachol	P value
secretion / cell (pC)	15.28±3.57	16.88±2.55	$p = 0.71$
number of non-overlapping events	42.88±7.20	71.83±7.4	* $p < 10^{-2}$
Q (pC)	0.26±0.02	0.19±0.01	* $p < 10^{-2}$
$Q^{1/3}$ ($pC^{1/3}$)	0.58±0.01	0.52±0.01	* $p < 10^{-3}$
spike amplitude (pA)	24.75±3.54	16.50±2.08	* $p < 0.05$
spike rise time (ms)	1.75±0.09	1.83±0.06	$p = 0.41$
spike halfwidth (ms)	7.40±0.33	7.63±0.25	$p = 0.57$
spike decay τ(ms)	15.47±1.01	15.10±0.59	$p = 0.73$
PSF amplitude (pA)	8.38±0.80	5.91±0.53	* $p < 10^{-2}$
PSF duration (ms)	5.75±0.48	5.24±0.29	$p = 0.34$
PSF area (fC)	24.52±2.63	16.05±1.39	* $p < 10^{-2}$

Table II:

Comparisons of the amperometric experimental results from chromaffin cells stimulated with 100 μM carbachol between the fructose-fed group and controls. The data in the control group was averaged from 34 cells obtained from 5 animals, and the data in the fructose-fed group was averaged from 38 cells obtained from 7animals.

	Control	Fructose-fed	P value
secretion / cell (pC)	15.28±3.57	16.86±3.68	$p = 0.76$
number of non-overlapping events	42.88±7.20	44.05±6.85	$p = 0.91$
Q (pC)	0.26±0.02	0.27±0.02	$p = 0.64$
$Q^{1/3}$ ($pC^{1/3}$)	0.58±0.01	0.58±0.01	$p = 0.99$
spike amplitude (pA)	24.75±3.54	36.18±4.59	$p = 0.06$
spike rise time (ms)	1.75±0.09	1.54±0.08	$p = 0.10$
spike halfwidth (ms)	7.40±0.33	6.20±0.30	* $p < 10^{-2}$
spike decay τ(ms)	15.47±1.01	13.05±0.83	$p = 0.07$
PSF amplitude (pA)	8.38±0.80	13.55±1.83	* $p < 0.05$
PSF duration (ms)	5.75±0.48	5.08±0.37	$p = 0.27$
PSF area (fC)	24.52±2.63	29.49±4.19	$p = 0.33$

Table III:

Comparisons of the amperometric experimental results from chromaffin cells in the control group when stimulated with 100 μM muscarine or 100 μM carbachol. The data from the 100 μM muscarine stimulation was averaged from 12 cells obtained from 2 rats, and the data from the 100 μM carbachol stimulation was averaged from 34 cells obtained from 5 animals.

Control	100 μM muscarine	100 μM carbachol	P value
secretion / cell (pC)	7.86±1.50	15.28±3.57	$p = 0.23$
number of non-overlapping events	35.92±7.50	42.88±7.20	$p = 0.59$
Q (pC)	0.23±0.03	0.26±0.02	$p = 0.51$
$Q^{1/3}$ ($pC^{1/3}$)	0.55±0.02	0.58±0.01	$p = 0.18$
spike amplitude (pA)	31.69±8.62	24.75±3.54	$p = 0.38$
spike rise time (ms)	1.54±0.14	1.75±0.09	$p = 0.26$
spike halfwidth (ms)	5.81±0.44	7.40±0.33	* $p < 0.05$
spike decay τ(ms)	14.58±1.48	15.47±1.01	$p = 0.64$
PSF amplitude (pA)	11.59±2.07	8.38±0.80	$p = 0.08$
PSF duration (ms)	6.01±0.63	5.75±0.48	$p = 0.77$
PSF area (fC)	30.54±4.62	24.52±2.63	$p = 0.25$

Table IV:

Comparisons of the amperometric experimental results from cells in the control group when stimulated with 100 μM muscarine or 100 μM DMPP. The data in the 100 μM muscarine stimulation was averaged from 12 cells obtained from 2 rats, and the data in the 100 μM DMPP stimulation was averaged from 49 cells obtained from 3 animals.

Control	100 μM muscarine	100 μM DMPP	P value
secretion / cell (pC)	7.86±1.50	13.53±1.89	$p = 0.15$
number of non-overlapping events	35.92±7.50	65.65±7.41	$p = 0.06$
Q (pC)	0.23±0.03	0.18±0.01	$p = 0.14$
$Q^{1/3}$ ($pC^{1/3}$)	0.55±0.02	0.50±0.01	$p = 0.09$
spike amplitude (pA)	31.69±8.62	17.49±1.84	* $p < 0.05$
spike rise time (ms)	1.54±0.14	1.78±0.05	$p = 0.06$
spike halfwidth (ms)	5.81±0.44	7.39±0.19	* $p < 10^{-3}$
spike decay τ(ms)	14.58±1.48	15.23±0.40	$p = 0.55$
PSF amplitude (pA)	11.59±2.07	6.38±0.56	* $p < 10^{-2}$
PSF duration (ms)	6.01±0.63	5.25±0.37	$p = 0.35$
PSF area (fC)	30.54±4.62	16.35±2.28	* $p < 10^{-2}$

Figures:

Figure I:

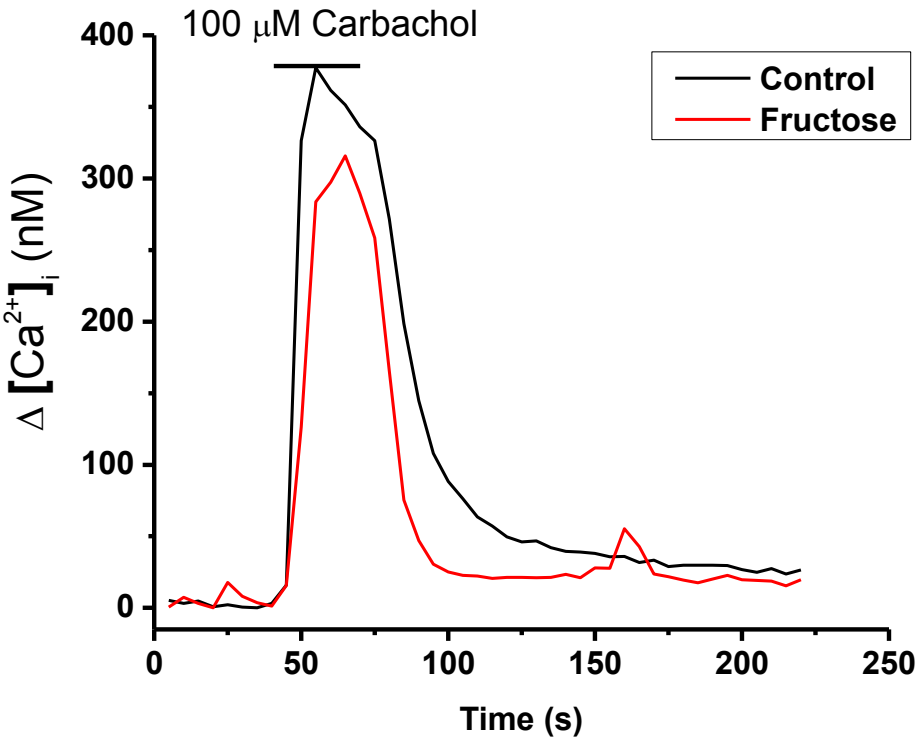

Changes in cytosolic [Ca^{2+}] when cells were stimulated with 100 uM carbachol. Fructose feeding reduced the amplitude of Ca^{2+} signal by ~14%. The mean time integral of the $[Ca^{2+}]_i$ rise was also decreased by ~27% via fructose feeding. Data averaged from 32 cells obtained from 2 rats in the control group and 19 cells from 2 rats in the fructose-fed group.

Figure II:

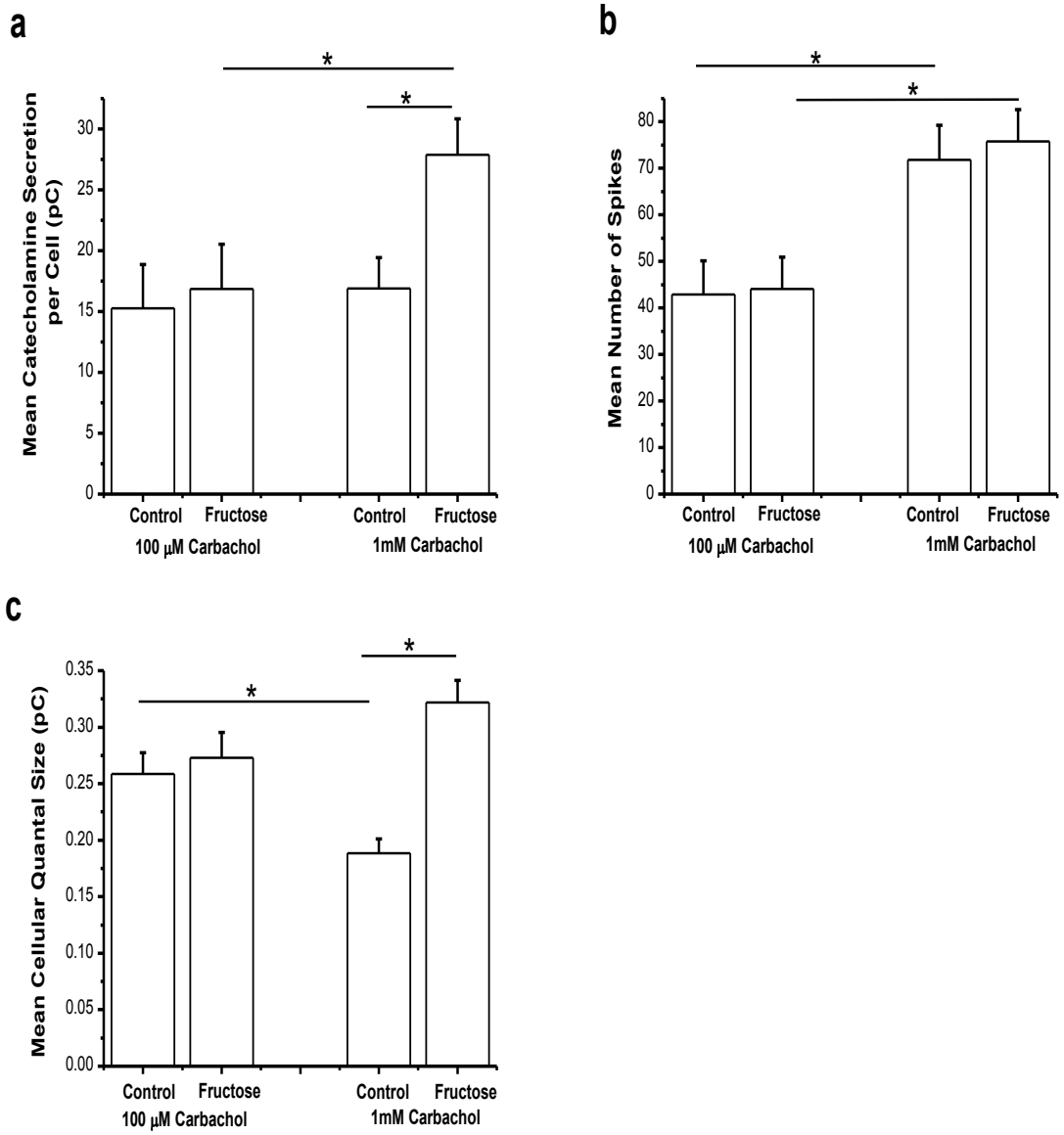

Comparison of fructose-induced effects in catecholamine secretion between 100 uM and 1 mM carbachol stimulation. Fructose feeding enhanced the secretion of catecholamine per cell and the mean cellular quantal size by a similar proportion when stimulated with 1 mM carbachol. These effects were not observed with the 100 μM carbachol stimulation.

Figure III:

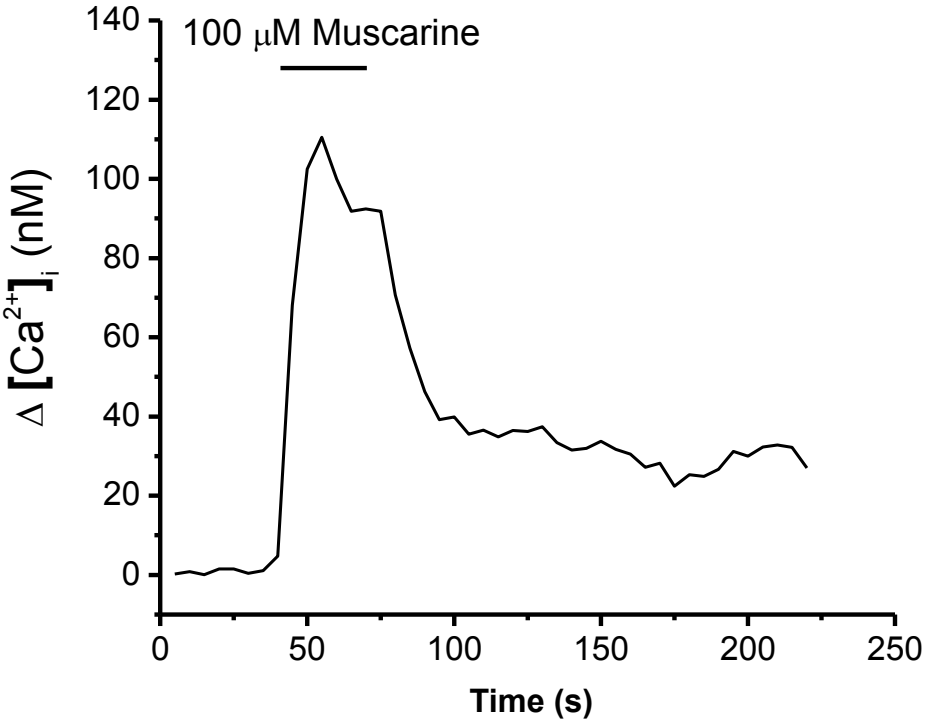

Changes in cytosolic [Ca^{2+}] when cells are stimulated with 100 μM muscarine. Data was averaged from 61 cells obtained from 2 control rats.

Reference List:

Alvarez, Y.D., L.I.Ibanez, O.D.Uchitel, and F.D.Marengo. 2008. P/Q Ca2+ channels are functionally coupled to exocytosis of the immediately releasable pool in mouse chromaffin cells. *Cell Calcium* 43:155-164.

Artalejo, C.R., M.E.Adams, and A.P.Fox. 1994. Three types of Ca2+ channel trigger secretion with different efficacies in chromaffin cells. *Nature* 367:72-76.

Augustine, G.J. and E.Neher. 1992. Calcium requirements for secretion in bovine chromaffin cells. *J. Physiol* 450:247-271.

Barbara, J.G., V.S.Lemos, and K.Takeda. 1998. Pre- and post-synaptic muscarinic receptors in thin slices of rat adrenal gland. *Eur. J. Neurosci.* 10:3535-3545.

Becherer, U., M.R.Medart, C.Schirra, E.Krause, D.Stevens, and J.Rettig. 2012. Regulated exocytosis in chromaffin cells and cytotoxic T lymphocytes: how similar are they? *Cell Calcium* 52:303-312.

Burgoyne, R.D. and A.Morgan. 1993. Regulated exocytosis. *Biochem. J.*

293 (Pt 2):305-316.

Burgoyne, R.D. and A.Morgan. 2003. Secretory granule exocytosis. *Physiol Rev.* 83:581-632.

Burgoyne, R.D. and A.Morgan. 1995. Ca2+ and secretory-vesicle dynamics. *Trends Neurosci.* 18:191-196.

Carabelli, V., A.Marcantoni, V.Comunanza, L.A.de, J.Diaz, R.Borges, and E.Carbone. 2007. Chronic hypoxia up-regulates alpha1H T-type channels and low-threshold catecholamine secretion in rat chromaffin cells. *J. Physiol* 584:149-165.

Chen, H.S., T.E.Wu, C.C.Juan, and H.D.Lin. 2009. Myocardial heat shock protein 60 expression in insulin-resistant and diabetic rats. *J. Endocrinol.* 200:151-157.

Chen, X.K., L.C.Wang, Y.Zhou, Q.Cai, M.Prakriya, K.L.Duan, Z.H.Sheng, C.Lingle, and Z.Zhou. 2005. Activation of GPCRs modulates quantal size in chromaffin cells through G(betagamma) and PKC. *Nat. Neurosci.* 8:1160-1168.

Chow, R.H., R.L.von, and E.Neher. 1992. Delay in vesicle fusion

revealed by electrochemical monitoring of single secretory events in adrenal chromaffin cells. *Nature* 356:60-63.

Cochilla, A.J., J.K.Angleson, and W.J.Betz. 2000. Differential regulation of granule-to-granule and granule-to-plasma membrane fusion during secretion from rat pituitary lactotrophs. *J. Cell Biol.* 150:839-848.

Colomer, C., C.Lafont, and N.C.Guerineau. 2008. Stress-induced intercellular communication remodeling in the rat adrenal medulla. *Ann. N. Y. Acad. Sci.* 1148:106-111.

Currie, K.P. 2010. Inhibition of Ca2+ channels and adrenal catecholamine release by G protein coupled receptors. *Cell Mol. Neurobiol.* 30:1201-1208.

Dodge, F.A., Jr. and R.Rahamimoff. 1967. Co-operative action a calcium ions in transmitter release at the neuromuscular junction. *J. Physiol* 193:419-432.

Elhamdani, A., H.C.Palfrey, and C.R.Artalejo. 2001. Quantal size is dependent on stimulation frequency and calcium entry in calf chromaffin cells. *Neuron* 31:819-830.

Engisch, K.L. and M.C.Nowycky. 1996. Calcium dependence of large dense-cored vesicle exocytosis evoked by calcium influx in bovine adrenal chromaffin cells. *J. Neurosci.* 16:1359-1369.

Fenwick, E.M., A.Marty, and E.Neher. 1982. A patch-clamp study of bovine chromaffin cells and of their sensitivity to acetylcholine. *J. Physiol* 331:577-597.

Floras, J.S. 2003. Sympathetic activation in human heart failure: diverse mechanisms, therapeutic opportunities. *Acta Physiol Scand.* 177:391-398.

Forsberg, E.J., E.Rojas, and H.B.Pollard. 1986. Muscarinic receptor enhancement of nicotine-induced catecholamine secretion may be mediated by phosphoinositide metabolism in bovine adrenal chromaffin cells. *J. Biol. Chem.* 261:4915-4920.

Giancippoli, A., M.Novara, L.A.de, P.Baldelli, A.Marcantoni, E.Carbone, and V.Carabelli. 2006. Low-threshold exocytosis induced by cAMP-recruited CaV3.2 (alpha1H) channels in rat chromaffin cells. *Biophys. J.* 90:1830-1841.

Gillis, K.D., R.Mossner, and E.Neher. 1996. Protein kinase C enhances exocytosis from chromaffin cells by increasing the size of the readily

releasable pool of secretory granules. *Neuron* 16:1209-1220.

Gong, L.W., I.Hafez, T.G.varez de, and M.Lindau. 2003. Secretory vesicles membrane area is regulated in tandem with quantal size in chromaffin cells. *J. Neurosci.* 23:7917-7921.

Guerineau, N.C., M.G.Desarmenien, V.Carabelli, and E.Carbone. 2012. Functional chromaffin cell plasticity in response to stress: focus on nicotinic, gap junction, and voltage-gated Ca2+ channels. *J. Mol. Neurosci.* 48:368-386.

Hanson, R.L., G.Imperatore, P.H.Bennett, and W.C.Knowler. 2002. Components of the "metabolic syndrome" and incidence of type 2 diabetes. *Diabetes* 51:3120-3127.

Hoppa, M.B., E.Jones, J.Karanauskaite, R.Ramracheya, M.Braun, S.C.Collins, Q.Zhang, A.Clark, L.Eliasson, C.Genoud, P.E.Macdonald, A.G.Monteith, S.Barg, J.Galvanovskis, and P.Rorsman. 2012. Multivesicular exocytosis in rat pancreatic beta cells. *Diabetologia* 55:1001-1012.

Hsieh, P.S. and W.C.Huang. 2001. Neonatal chemical sympathectomy attenuates fructose-induced hypertriglyceridemia and hypertension in rats.

Chin J. Physiol 44:25-31.

Hwang, I.S., H.Ho, B.B.Hoffman, and G.M.Reaven. 1987. Fructose-induced insulin resistance and hypertension in rats. *Hypertension* 10:512-516.

Kamide, K., H.Rakugi, J.Higaki, A.Okamura, M.Nagai, K.Moriguchi, M.Ohishi, N.Satoh, M.L.Tuck, and T.Ogihara. 2002. The renin-angiotensin and adrenergic nervous system in cardiac hypertrophy in fructose-fed rats. *Am. J. Hypertens.* 15:66-71.

Kao, L.S. and A.S.Schneider. 1985. Muscarinic receptors on bovine chromaffin cells mediate a rise in cytosolic calcium that is independent of extracellular calcium. *J. Biol. Chem.* 260:2019-2022.

Kilpatrick, D.L., R.J.Slepetis, J.J.Corcoran, and N.Kirshner. 1982. Calcium uptake and catecholamine secretion by cultured bovine adrenal medulla cells. *J. Neurochem.* 38:427-435.

Kleinle, J., K.Vogt, H.R.Luscher, L.Muller, W.Senn, K.Wyler, and J.Streit. 1996. Transmitter concentration profiles in the synaptic cleft: an analytical model of release and diffusion. *Biophys. J.* 71:2413-2426.

Klenchin, V.A. and T.F.Martin. 2000. Priming in exocytosis: attaining fusion-competence after vesicle docking. *Biochimie* 82:399-407.

Kvetnansky, R., E.L.Sabban, and M.Palkovits. 2009. Catecholaminergic systems in stress: structural and molecular genetic approaches. *Physiol Rev.* 89:535-606.

Lorenzo, C., M.Okoloise, K.Williams, M.P.Stern, and S.M.Haffner. 2003. The metabolic syndrome as predictor of type 2 diabetes: the San Antonio heart study. *Diabetes Care* 26:3153-3159.

Lou, P.H., E.Lucchinetti, L.Zhang, A.Affolter, M.Gandhi, A.Zhakupova, M.Hersberger, T.Hornemann, A.S.Clanachan, and M.Zaugg. 2015. Propofol (Diprivan(R)) and Intralipid(R) exacerbate insulin resistance in type-2 diabetic hearts by impairing GLUT4 trafficking. *Anesth. Analg.* 120:329-340.

Lukyanetz, E.A. and E.Neher. 1999. Different types of calcium channels and secretion from bovine chromaffin cells. *Eur. J. Neurosci.* 11:2865-2873.

Machado, J.D., A.Morales, J.F.Gomez, and R.Borges. 2001. cAmp modulates exocytotic kinetics and increases quantal size in chromaffin

cells. *Mol. Pharmacol.* 60:514-520.

Matthews-Bellinger, J. and M.M.Salpeter. 1978. Distribution of acetylcholine receptors at frog neuromuscular junctions with a discussion of some physiological implications. *J. Physiol* 279:197-213.

Miranda-Ferreira, R., P.R.de, A.M.de Diego, A.Caricati-Neto, L.Gandia, A.Jurkiewicz, and A.G.Garcia. 2008. Single-vesicle catecholamine release has greater quantal content and faster kinetics in chromaffin cells from hypertensive, as compared with normotensive, rats. *J. Pharmacol. Exp. Ther.* 324:685-693.

Morgan, A. and R.D.Burgoyne. 1997. Common mechanisms for regulated exocytosis in the chromaffin cell and the synapse. *Semin. Cell Dev. Biol.* 8:141-149.

Mosharov, E.V. and D.Sulzer. 2005. Analysis of exocytotic events recorded by amperometry. *Nat. Methods* 2:651-658.

Nagy, G., U.Matti, R.B.Nehring, T.Binz, J.Rettig, E.Neher, and J.B.Sorensen. 2002. Protein kinase C-dependent phosphorylation of synaptosome-associated protein of 25 kDa at Ser187 potentiates vesicle recruitment. *J. Neurosci.* 22:9278-9286.

Novara, M., P.Baldelli, D.Cavallari, V.Carabelli, A.Giancippoli, and E.Carbone. 2004. Exposure to cAMP and beta-adrenergic stimulation recruits Ca(V)3 T-type channels in rat chromaffin cells through Epac cAMP-receptor proteins. *J. Physiol* 558:433-449.

Panchal, S.K. and L.Brown. 2011. Rodent models for metabolic syndrome research. *J. Biomed. Biotechnol.* 2011:351982.

Rettig, J. and E.Neher. 2002. Emerging roles of presynaptic proteins in Ca++-triggered exocytosis. *Science* 298:781-785.

Schneider, A.S., R.Herz, and K.Rosenheck. 1977. Stimulus-secretion coupling in chromaffin cells isolated from bovine adrenal medulla. *Proc. Natl. Acad. Sci. U. S. A* 74:5036-5040.

Shirvan, M.H., H.B.Pollard, and E.Heldman. 1991. Mixed nicotinic and muscarinic features of cholinergic receptor coupled to secretion in bovine chromaffin cells. *Proc. Natl. Acad. Sci. U. S. A* 88:4860-4864.

Smart, J.L. and J.A.McCammon. 1998. Analysis of synaptic transmission in the neuromuscular junction using a continuum finite element model. *Biophys. J.* 75:1679-1688.

Smith, C. 1999. A persistent activity-dependent facilitation in chromaffin cells is caused by Ca2+ activation of protein kinase C. *J. Neurosci.* 19:589-598.

Takiyyuddin, M.A., N.L.De, F.B.Gabbai, T.Q.Dinh, B.Kennedy, M.G.Ziegler, E.L.Sabban, R.J.Parmer, and D.T.O'Connor. 1993. Catecholamine secretory vesicles. Augmented chromogranins and amines in secondary hypertension. *Hypertension* 21:674-679.

Tang, K.S., A.Tse, and F.W.Tse. 2005. Differential regulation of multiple populations of granules in rat adrenal chromaffin cells by culture duration and cyclic AMP. *J. Neurochem.* 92:1126-1139.

Toledo G., R.Fernandez-Chacon, and J.M.Fernandez. 1993. Release of secretory products during transient vesicle fusion. *Nature* 363:554-558.

Tran, L.T., V.G.Yuen, and J.H.McNeill. 2009. The fructose-fed rat: a review on the mechanisms of fructose-induced insulin resistance and hypertension. *Mol. Cell Biochem.* 332:145-159.

Trifaro, J.M. and M.L.Vitale. 1993. Cytoskeleton dynamics during neurotransmitter release. *Trends Neurosci.* 16:466-472.

Verma, S., S.Bhanot, and J.H.McNeill. 1999. Sympathectomy prevents fructose-induced hyperinsulinemia and hypertension. *Eur. J. Pharmacol.* 373:R1-R4.

Wajchenberg, B.L., D.A.Malerbi, M.S.Rocha, A.C.Lerario, and A.T.Santomauro. 1994. Syndrome X: a syndrome of insulin resistance. Epidemiological and clinical evidence. *Diabetes Metab Rev.* 10:19-29.

Wang, N., C.Kwan, X.Gong, E.P.de Chaves, A.Tse, and F.W.Tse. 2010. Influence of cholesterol on catecholamine release from the fusion pore of large dense core chromaffin granules. *J. Neurosci.* 30:3904-3911.

Warren, B.E., P.H.Lou, E.Lucchinetti, L.Zhang, A.S.Clanachan, A.Affolter, M.Hersberger, M.Zaugg, and H.Lemieux. 2014. Early mitochondrial dysfunction in glycolytic muscle, but not oxidative muscle, of the fructose-fed insulin-resistant rat. *Am. J. Physiol Endocrinol. Metab* 306:E658-E667.

Wu, P.C., M.J.Fann, and L.S.Kao. 2010. Characterization of Ca2+ signaling pathways in mouse adrenal medullary chromaffin cells. *J. Neurochem.* 112:1210-1222.

Xu, J. and F.W.Tse. 1999. Brefeldin A increases the quantal size and alters

the kinetics of catecholamine release from rat adrenal chromaffin cells. *J. Biol. Chem.* 274:19095-19102.

Yuan, G., J.Nanduri, S.Khan, G.L.Semenza, and N.R.Prabhakar. 2008. Induction of HIF-1alpha expression by intermittent hypoxia: involvement of NADPH oxidase, Ca2+ signaling, prolyl hydroxylases, and mTOR. *J. Cell Physiol* 217:674-685.

Zhang, J., R.Xue, W.Y.Ong, and P.Chen. 2009. Roles of cholesterol in vesicle fusion and motion. *Biophys. J.* 97:1371-1380.

Zhou, Z. and S.Misler. 1995. Action potential-induced quantal secretion of catecholamines from rat adrenal chromaffin cells. *J. Biol. Chem.* 270:3498-3505.

Zhou, Z., S.Misler, and R.H.Chow. 1996. Rapid fluctuations in transmitter release from single vesicles in bovine adrenal chromaffin cells. *Biophys. J.* 70:1543-1552.